# Using Microseismicity to Image the Structure of the Basel Geothermal Reservoir

A. Reshetnikov[1], J. Kummerow[1], S. A. Shapiro[1], H. Asanuma[2], and M. Häring[3]

[1] Freie Universität Berlin
[2] Tohoku University
[3] Geothermal Explorers International Ltd

May 24, 2011

# Outline

- Basel microseismic data
- Microseismic reflection imaging approach
- Large scale fault system image
- Image of the microseismic cloud interior

# Basel microseismic data

~2000 events, 4 stations

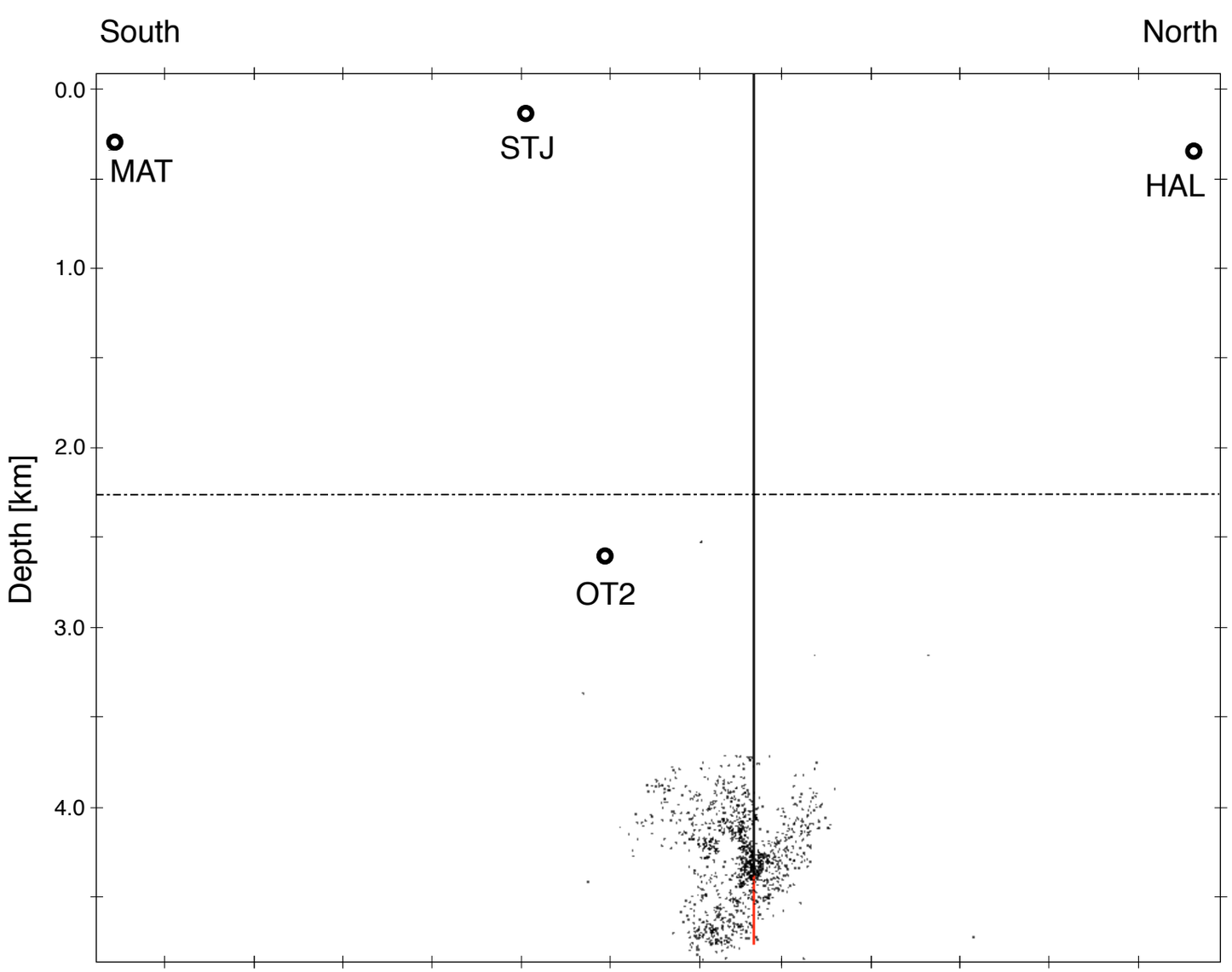


Side view

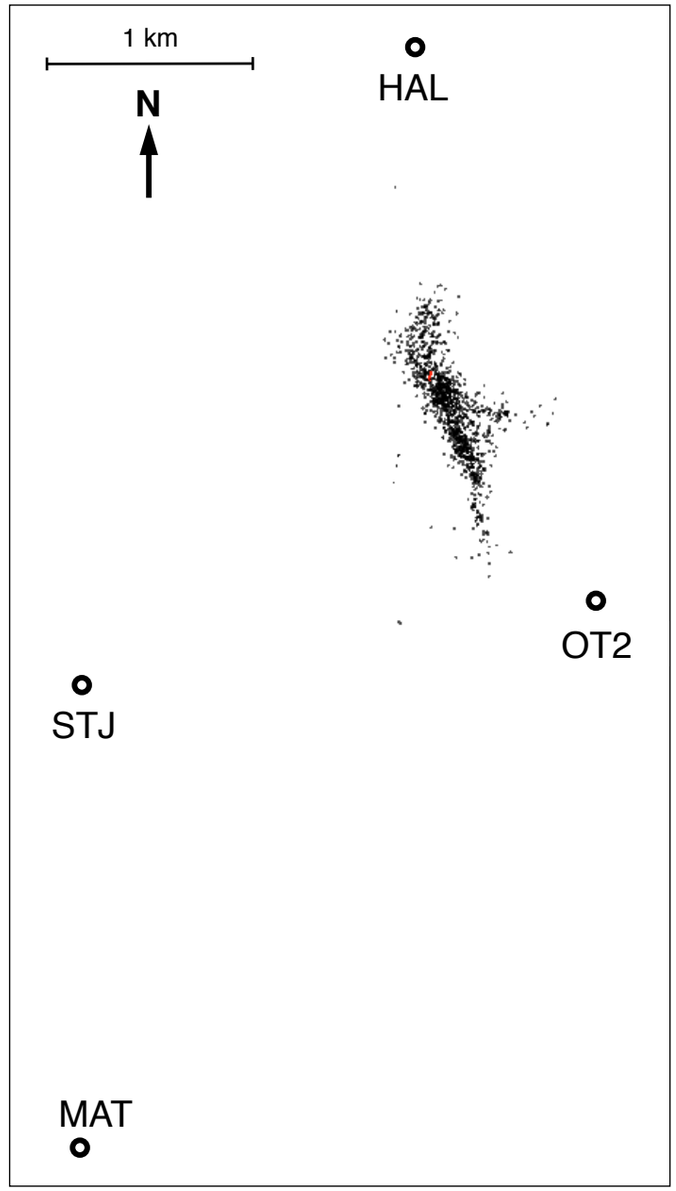


Map view

**Wed 25, 14:20 P193.** J. Kummerow, S. A. Shapiro, H. Asanuma, and M. Häring. Application of an Arrival Time and Cross Correlation Value-based Location Algorithm to the Basel Microseismic Data

# Basel microseismic data

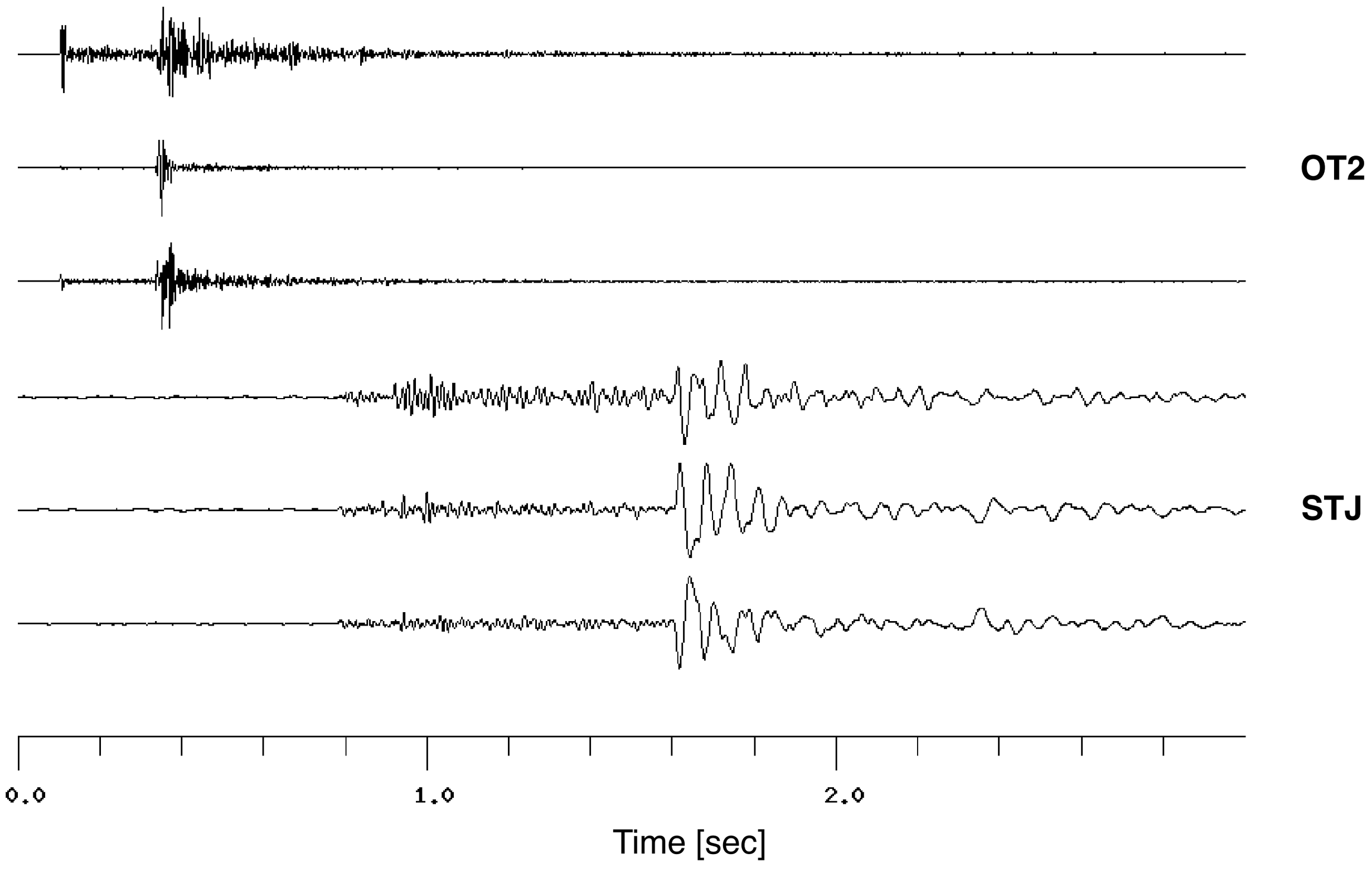

# Basel microseismic data

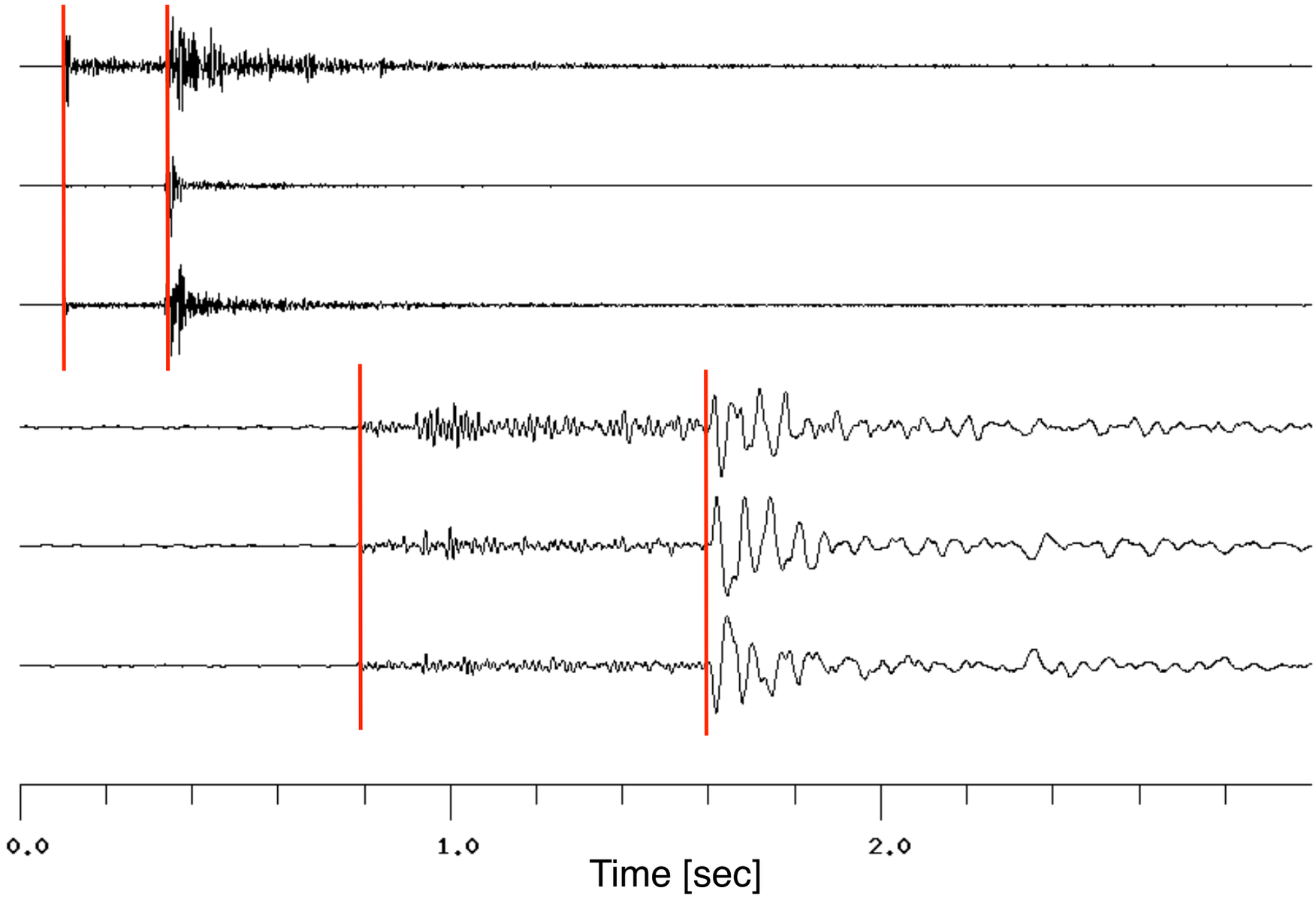


**OT2**:
2300 P and S hand picks

**STJ**:
1500 P and S hand picks

# Basel microseismic data

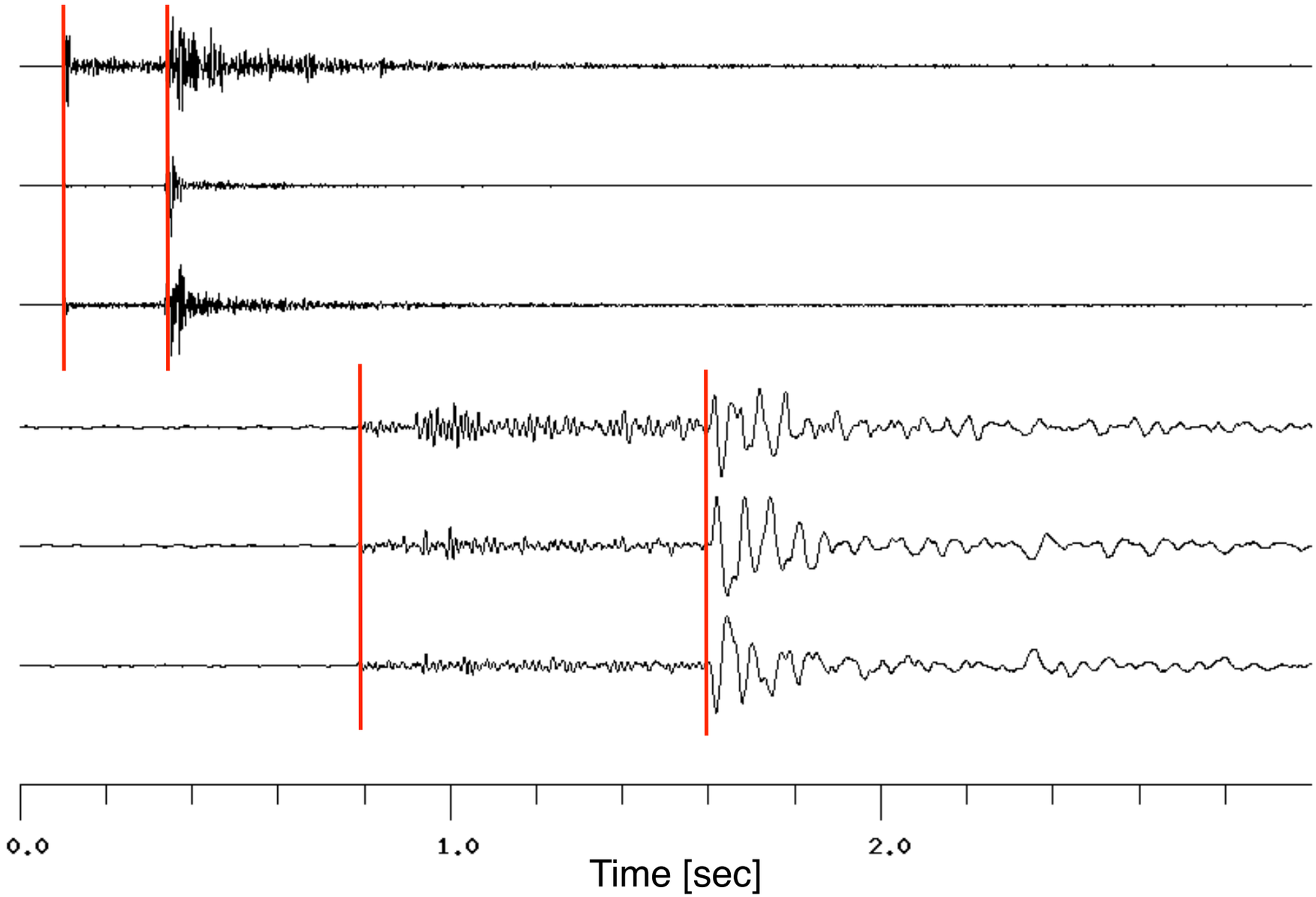


**OT2**:
2300 P and S hand picks

**STJ**:
1500 P and S hand picks

**Location procedure** ⟶

- Event coordinates
- Event triggering time
- Residuals for each station
- RMS misfit

# Basel microseismic data

Number of P- and S- hand picks:

**OT2**: ~2300
**STJ**: ~1500
**MAT**: ~2100
**HAL**: ~1750

**Event selection criteria:**

- S/N ratio
- residual
- RMS misfit

→

**OT2**: 600 events

**STJ**: 850 events

**MAT**: 720 events

**HAL**: 450 events

# Basel microseismic data: frequency spectra

**Signal** ——

**Noise** ——

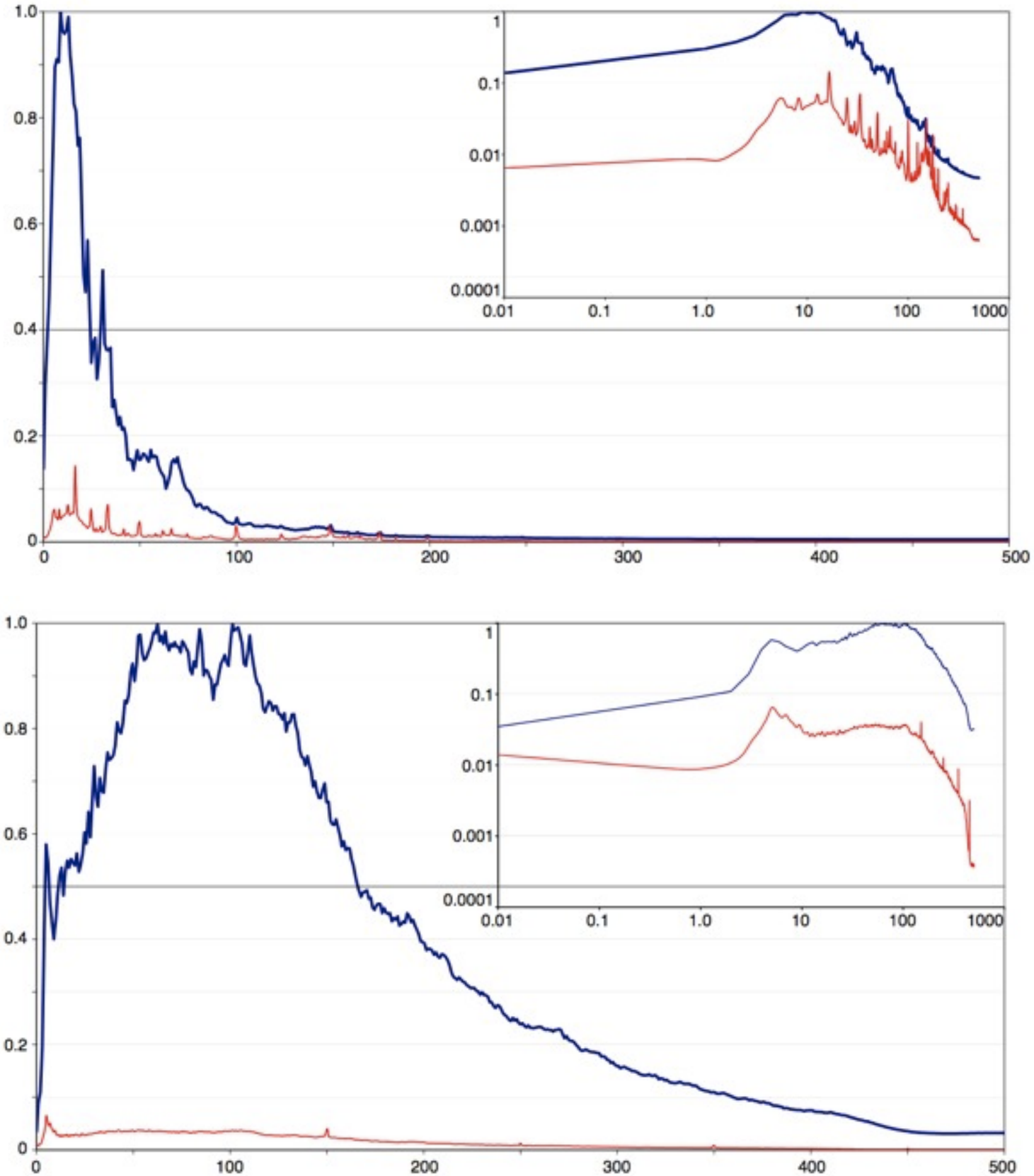


**STJ**




**OT2**

# Microseismic reflection imaging

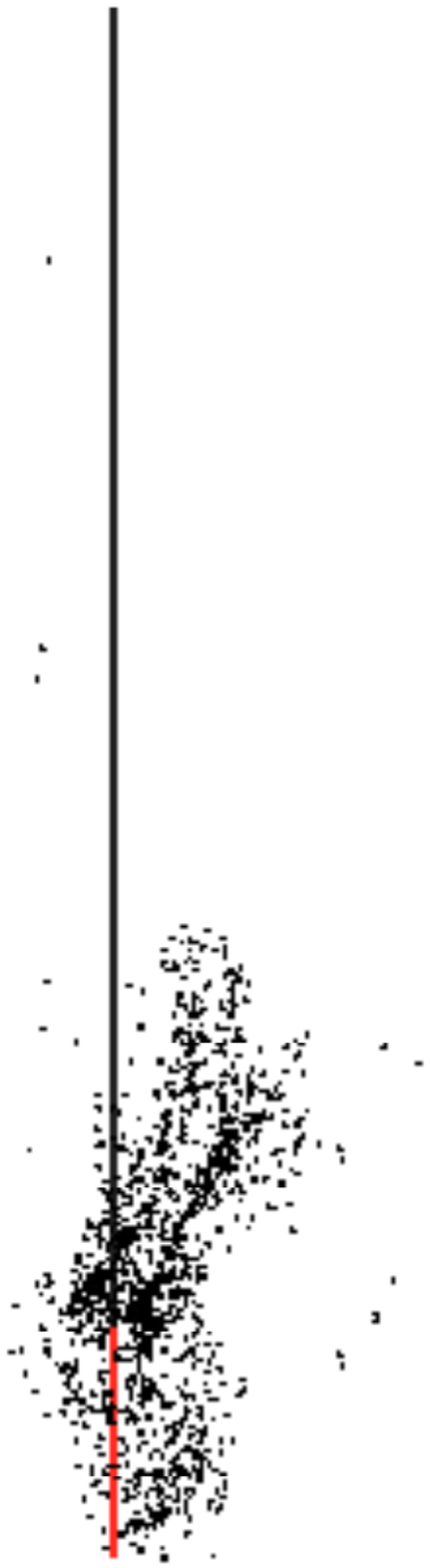

Geophone

- Single borehole geophone
- Cloud of microseismicity

- Single source
- Cloud of spatially distributed receivers

# Common shot gather form a microseismic cloud

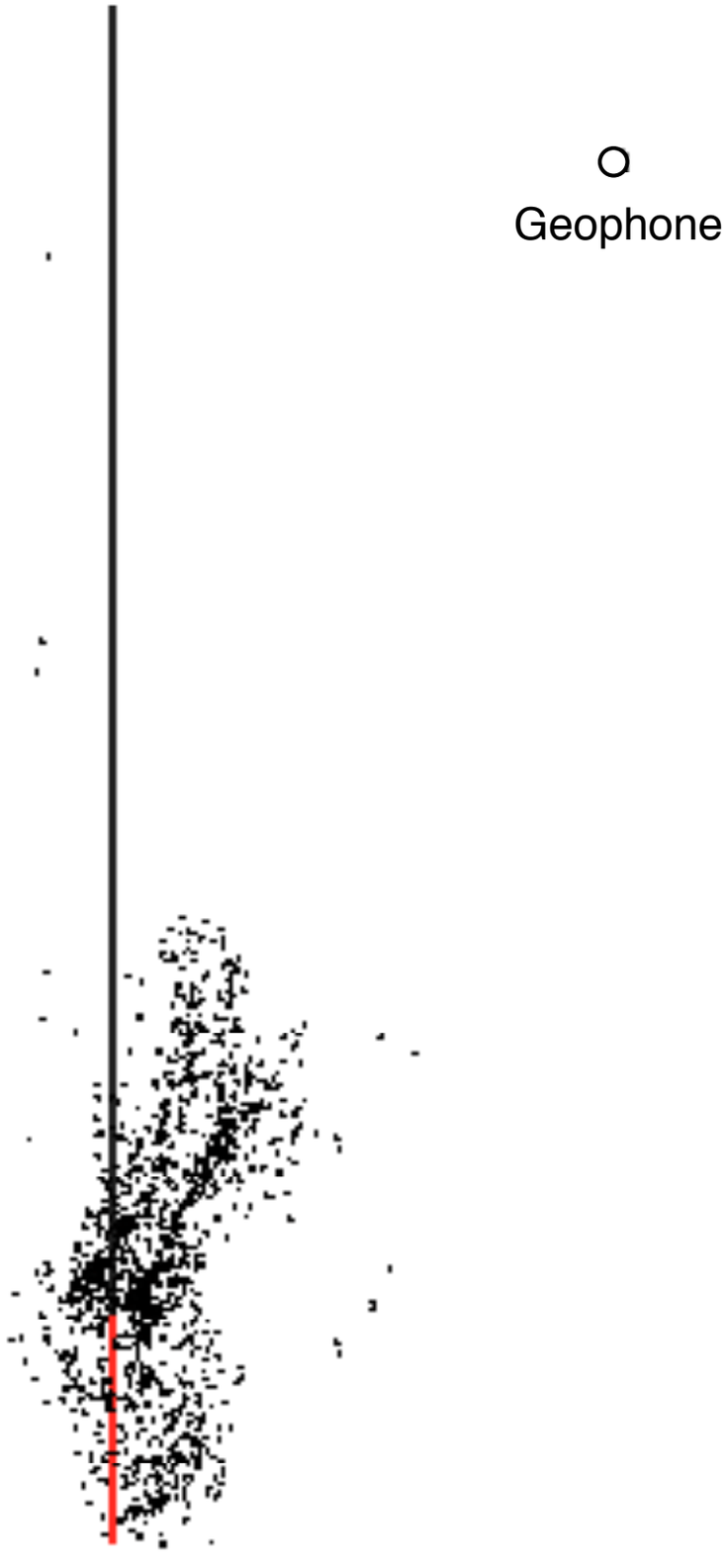


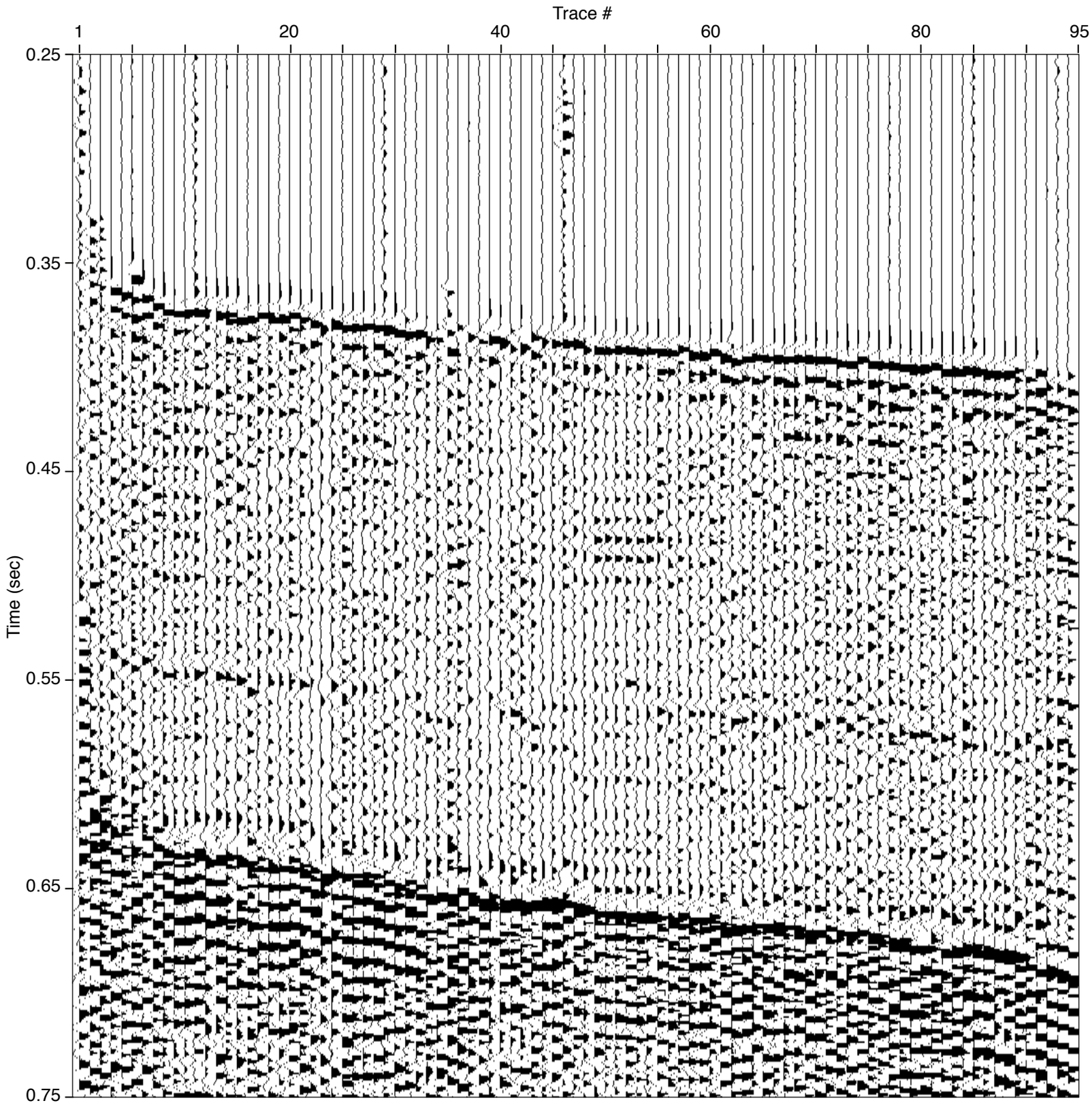

# Imaging procedure

**Basis:** 3D Kirchhoff prestack depth migration

**Principle:** restriction of migration operator to the region around the actual reflection point

**Benefits:** improved image quality and better resolution (less artefacts), in particular, for low fold and steeply dipping reflectors

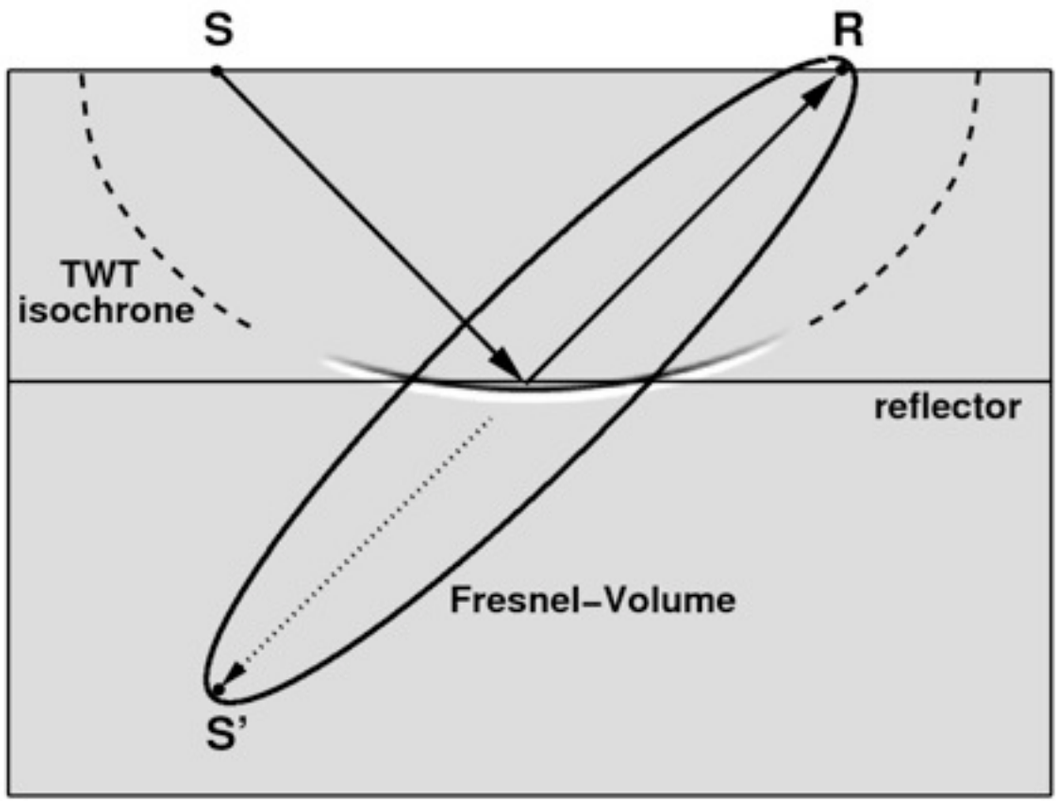


Buske et al. (2006)

# Geophone azimuthal orientation

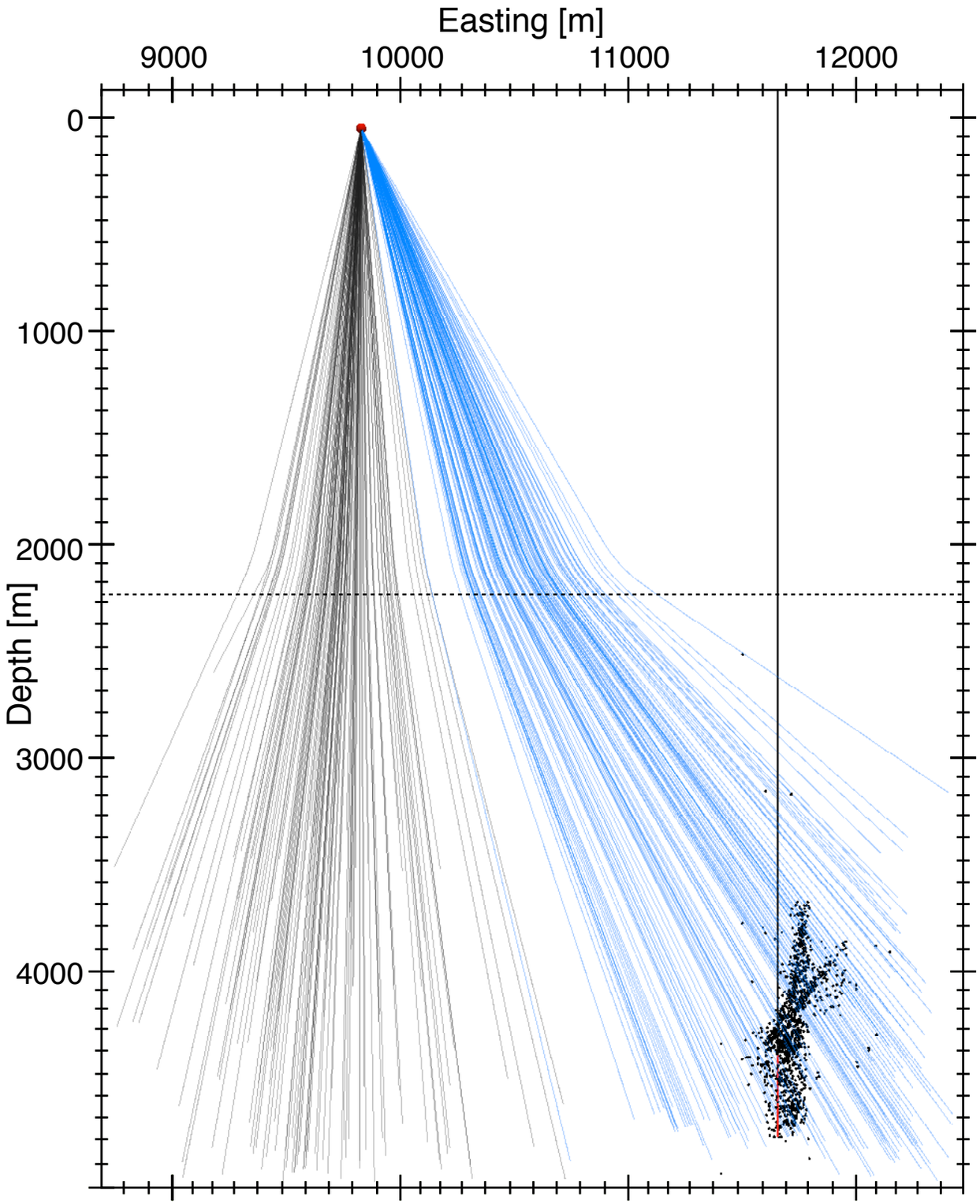


Side view

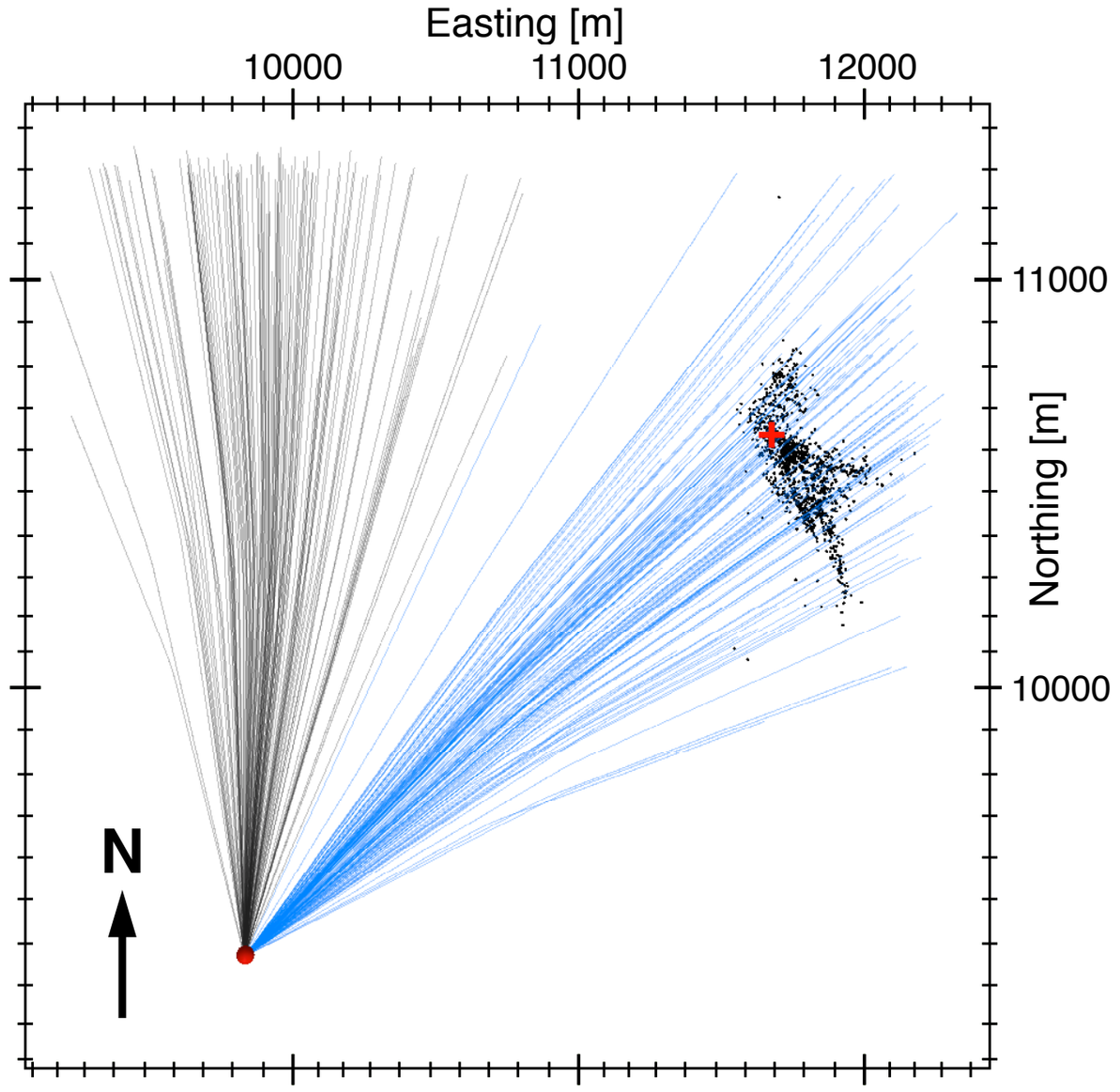


Map view

# Geophone azimuthal orientation

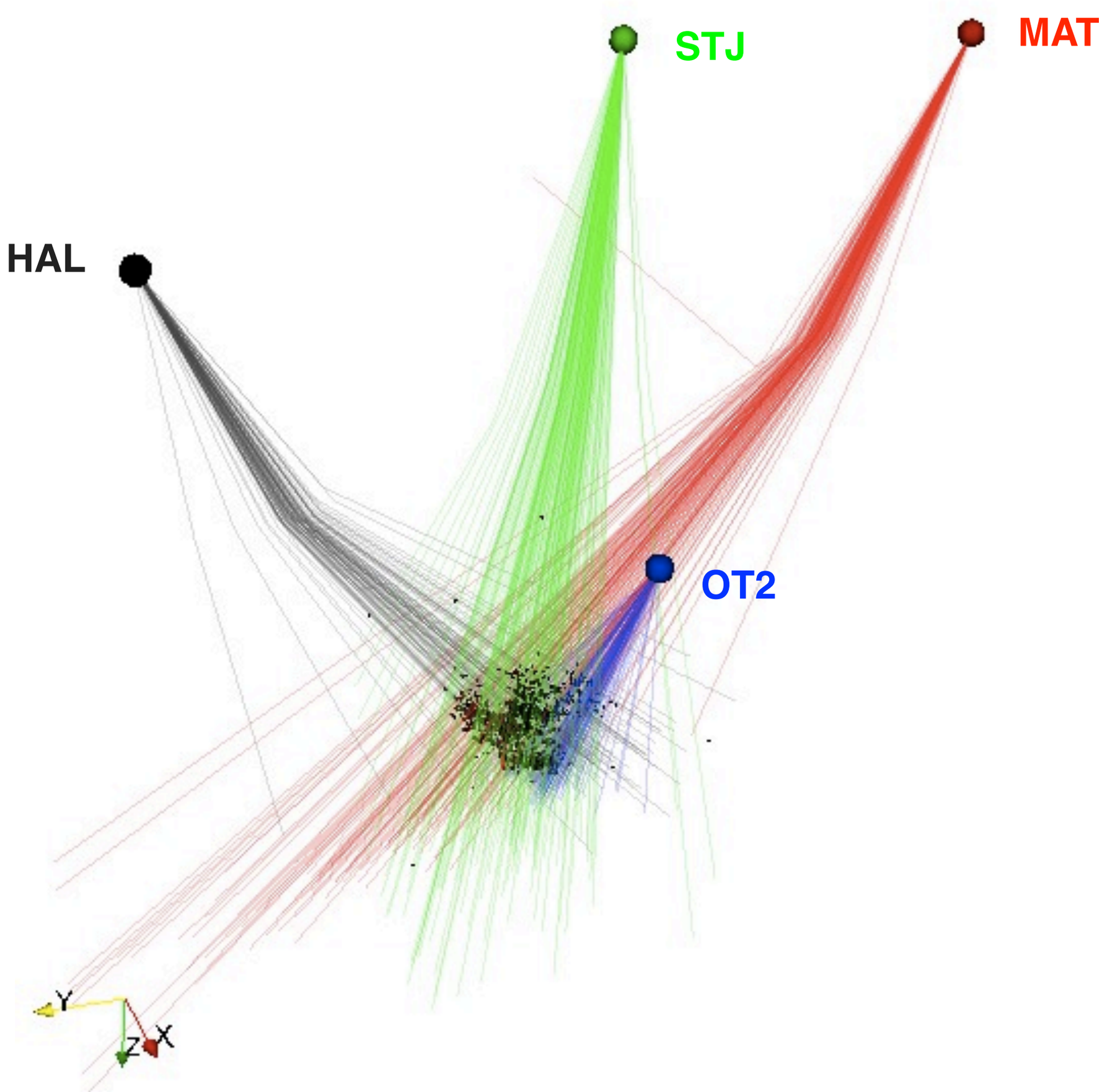

# Large scale fault system image

600 microseismic events

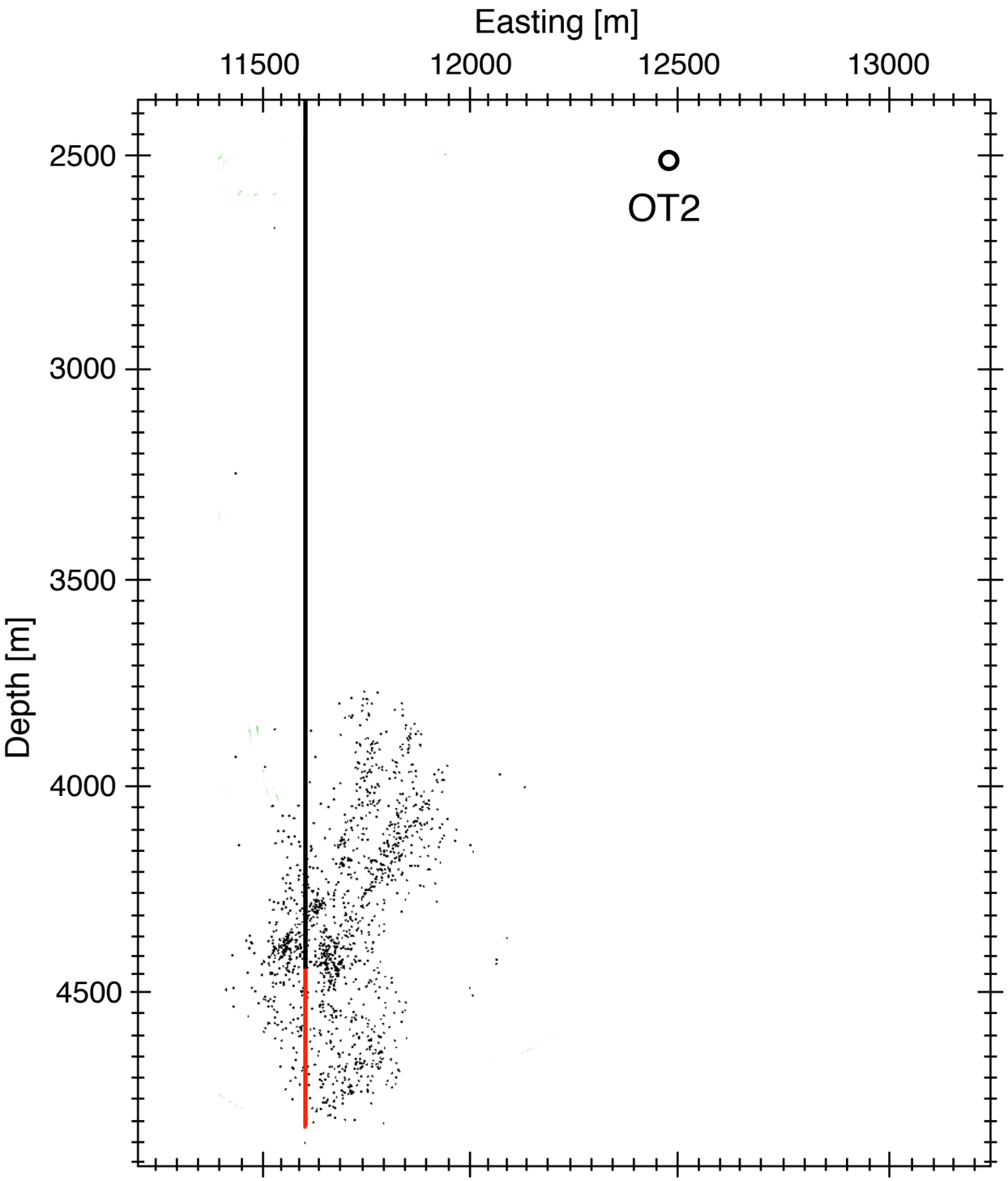


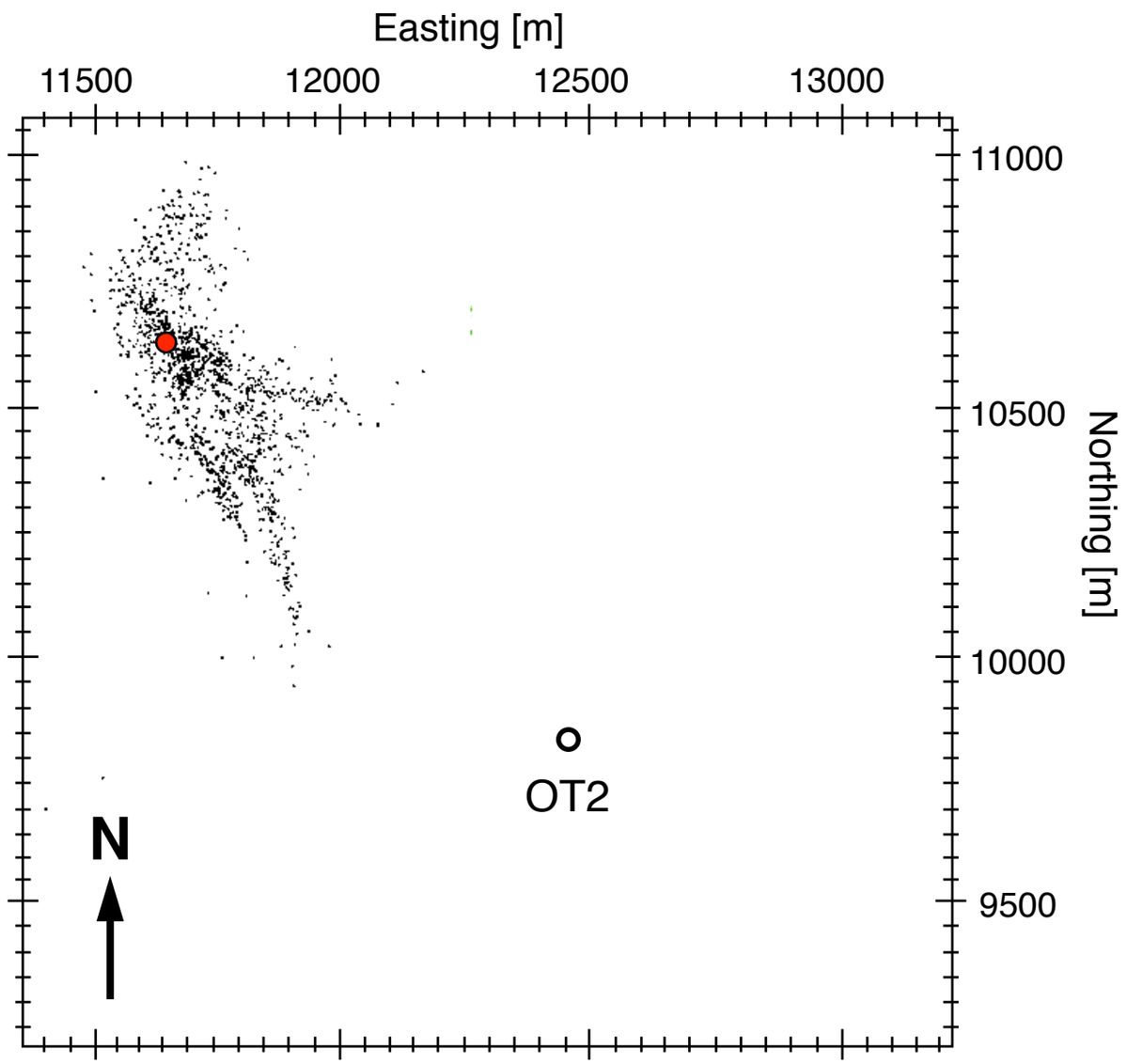

# Large scale fault system image

600 microseismic events

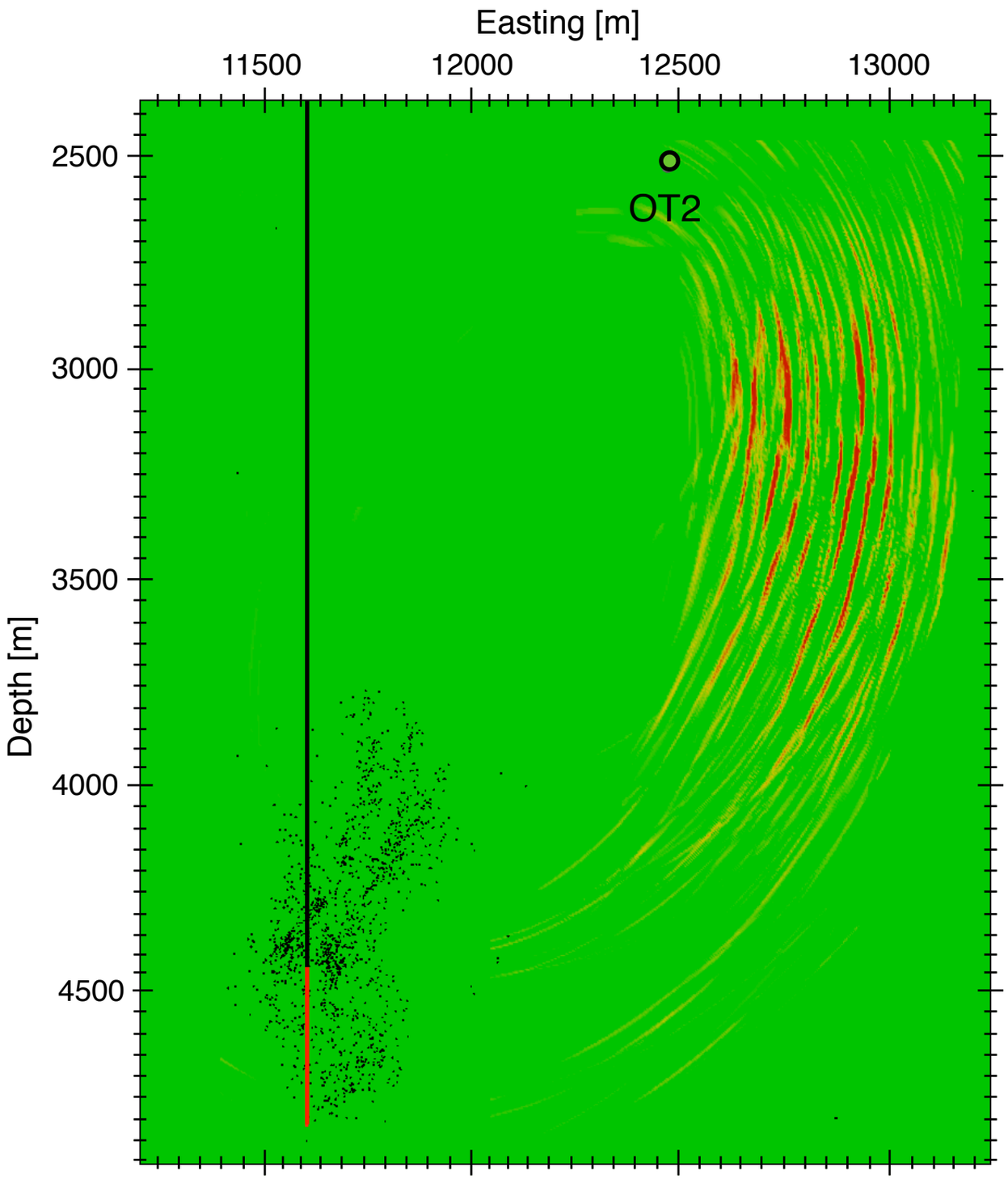


Vertical section

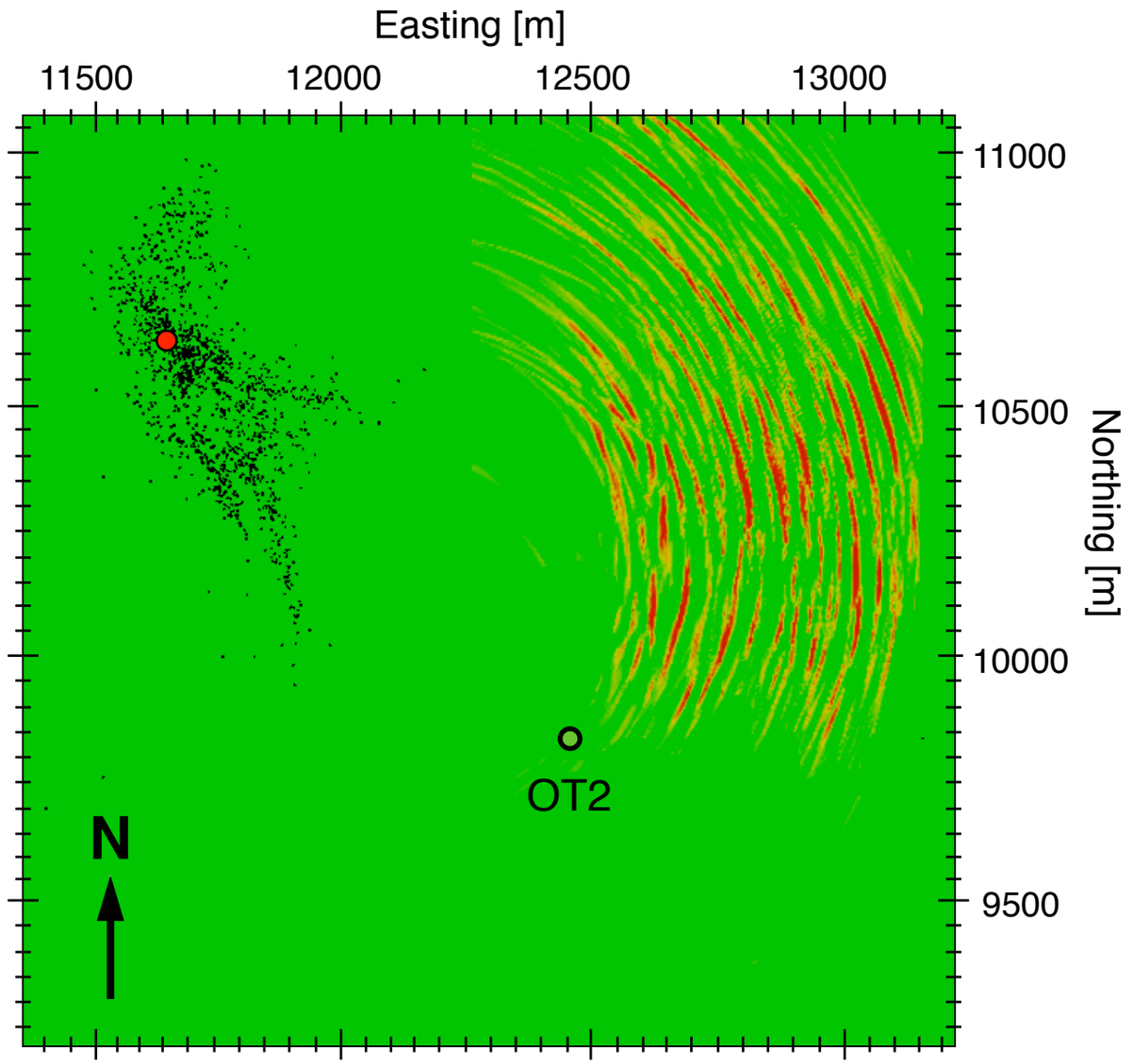


Horizontal section

# Large scale fault system image

600 microseismic events

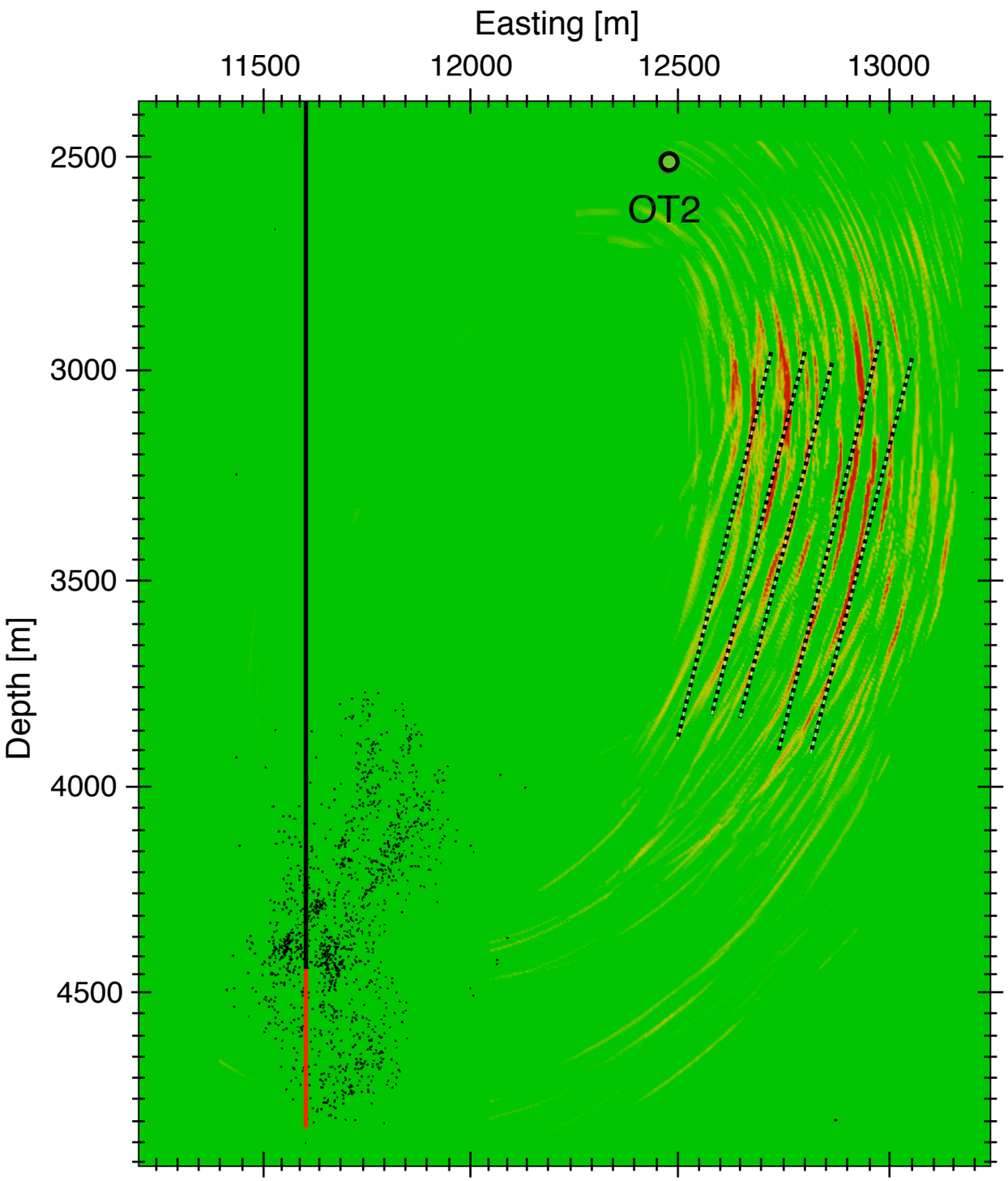


Vertical section

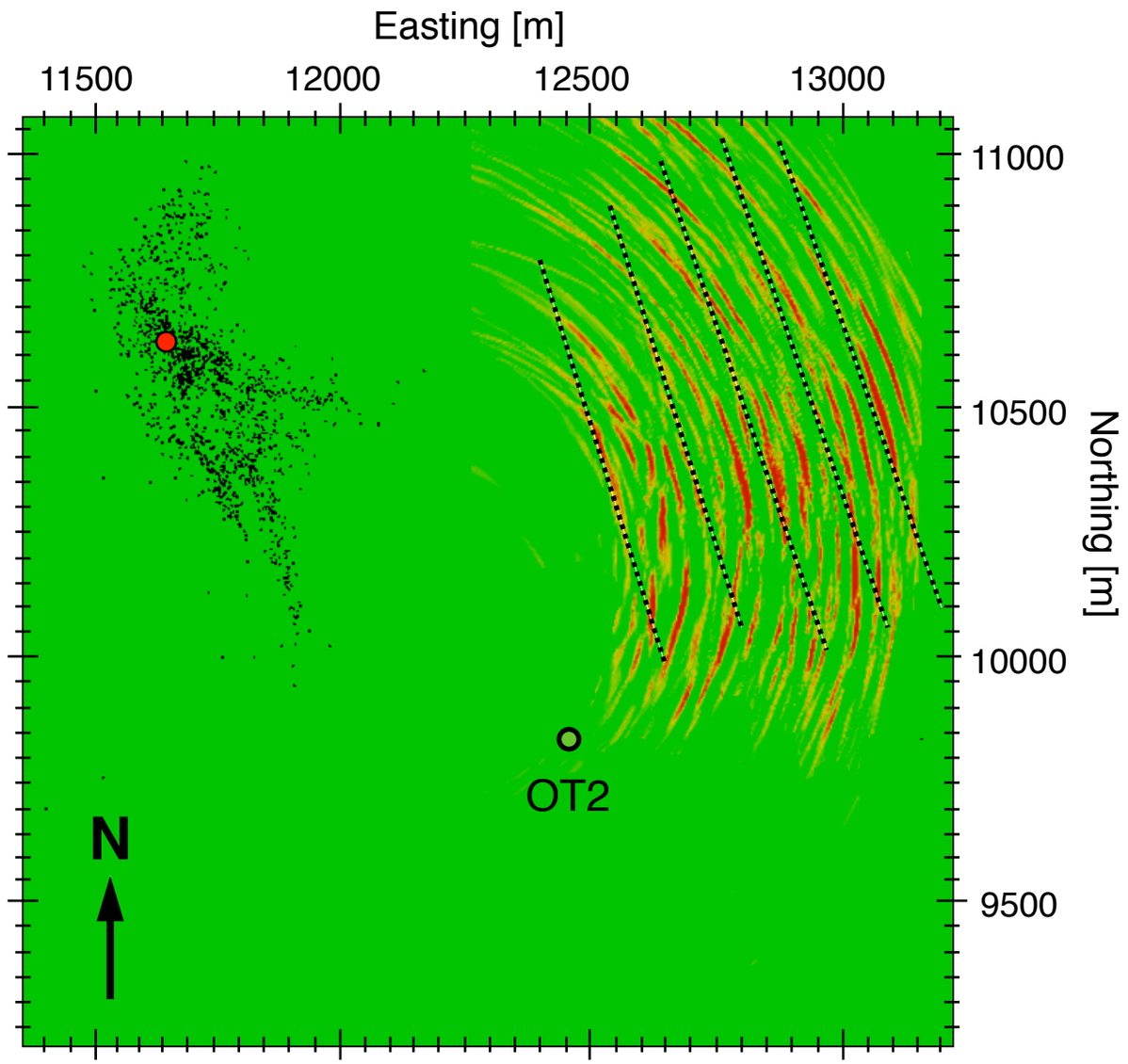


Horizontal section

# Results from Dyer et al. (2008)

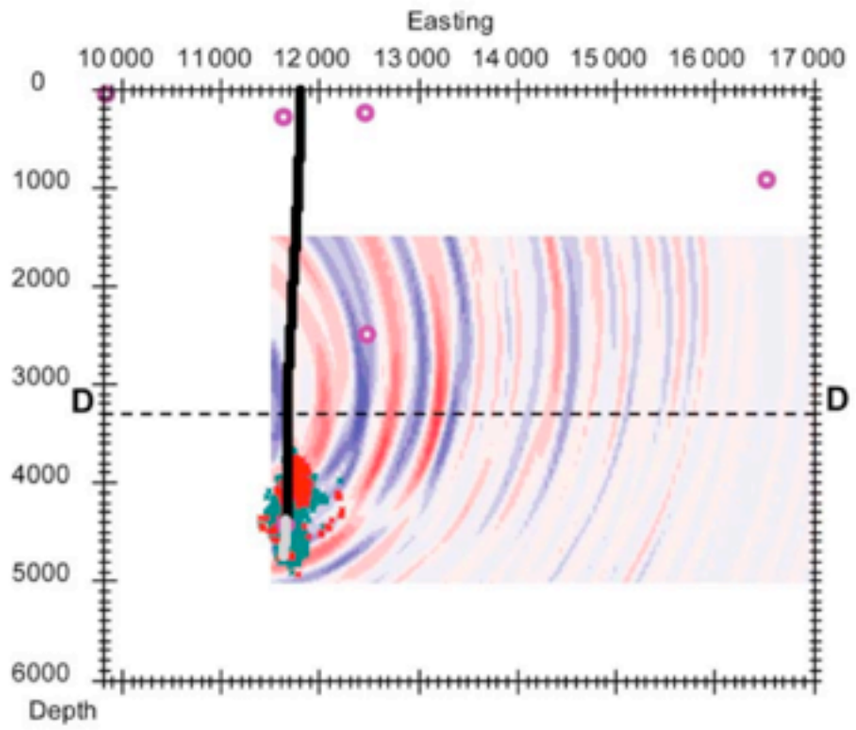


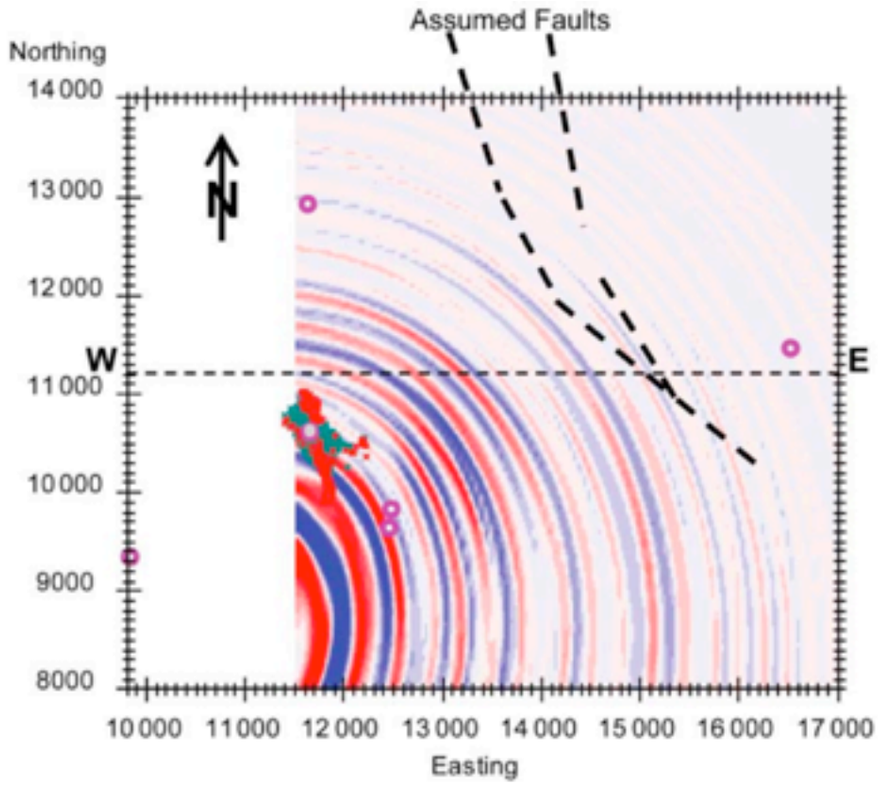


Original image

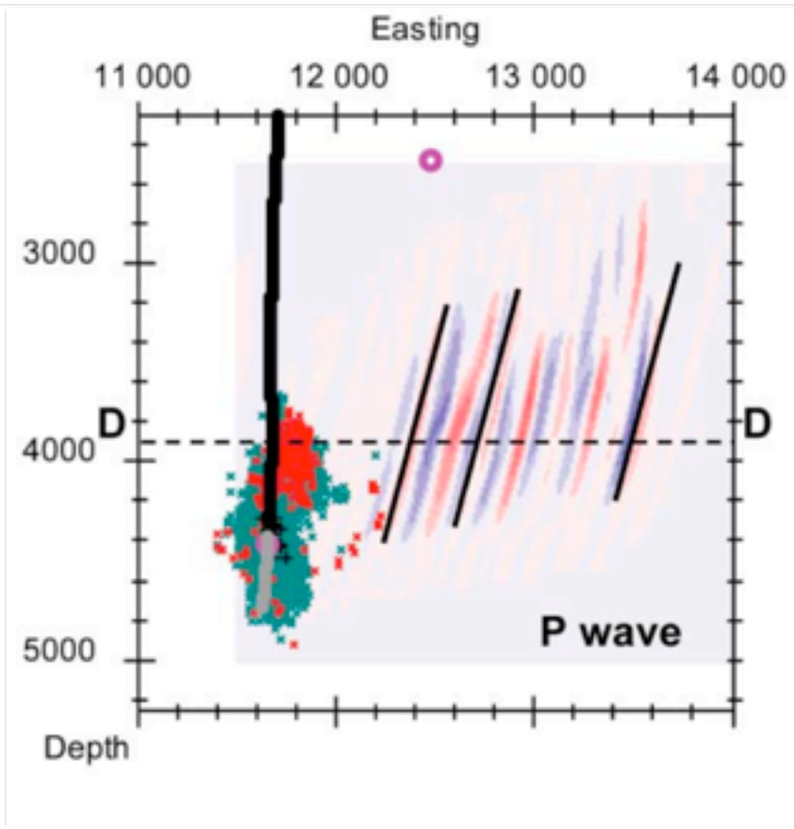


Vertical section

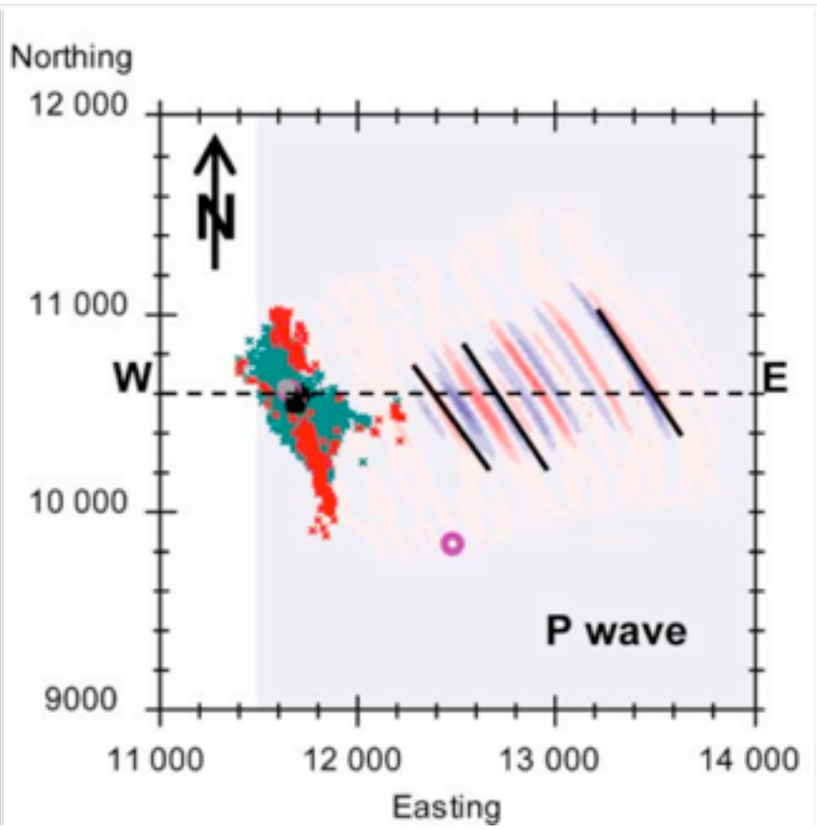


Horizontal section

Image with aperture control

# Results from Dyer et al. (2008)

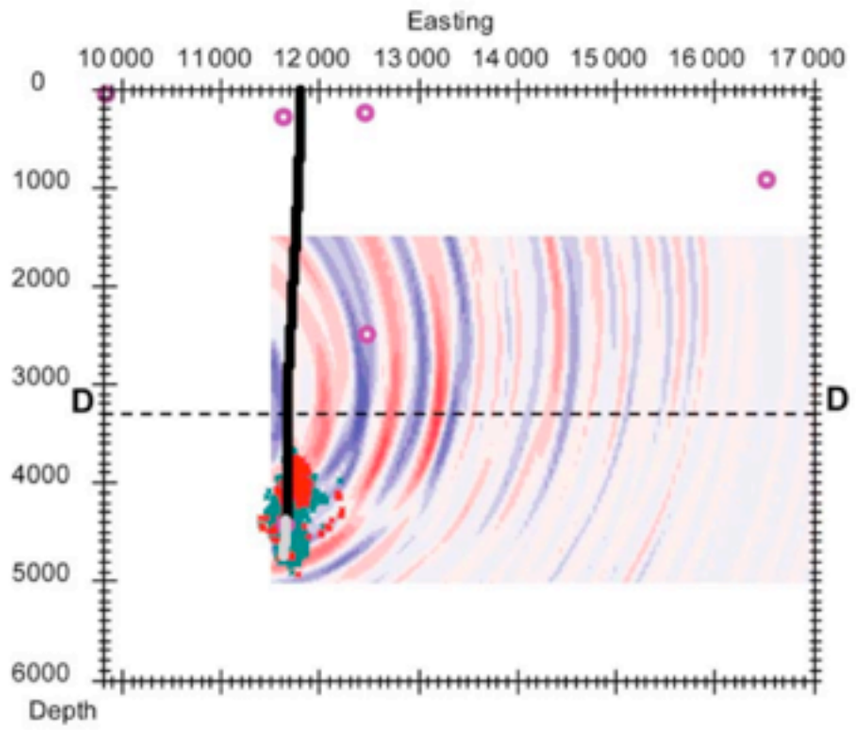


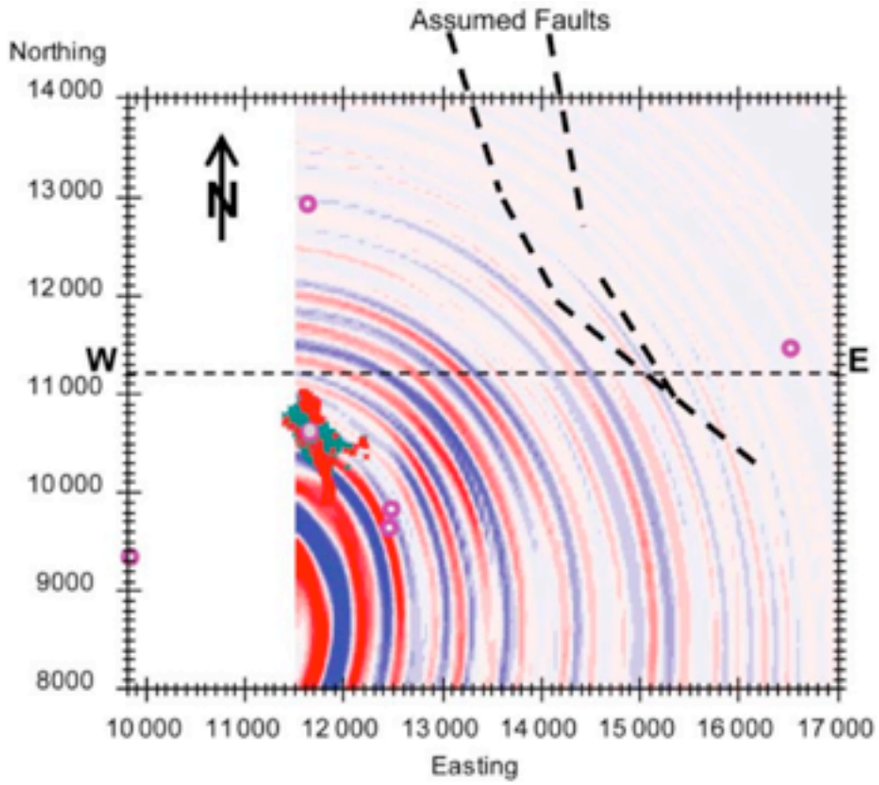


Original image

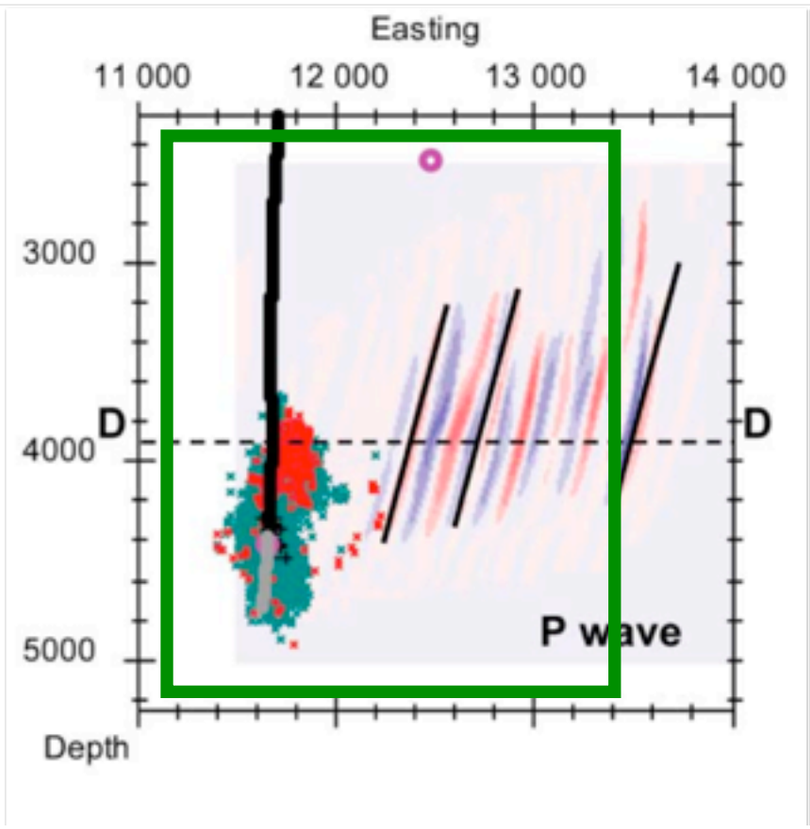


Vertical section

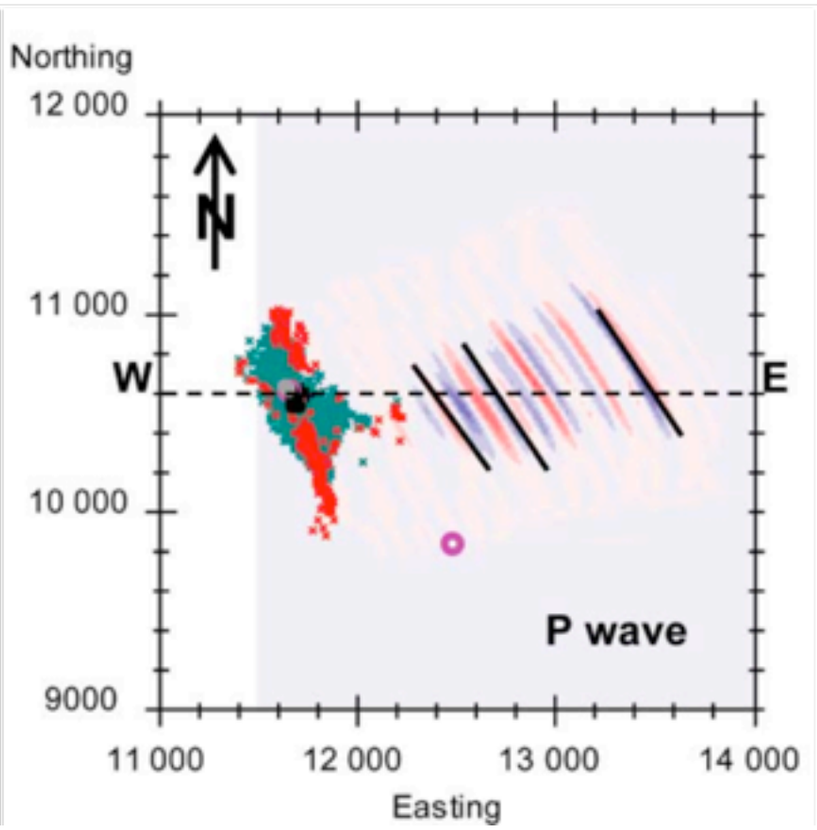


Horizontal section

Image with aperture control

# Large scale fault system image: comparison

Vertical sections

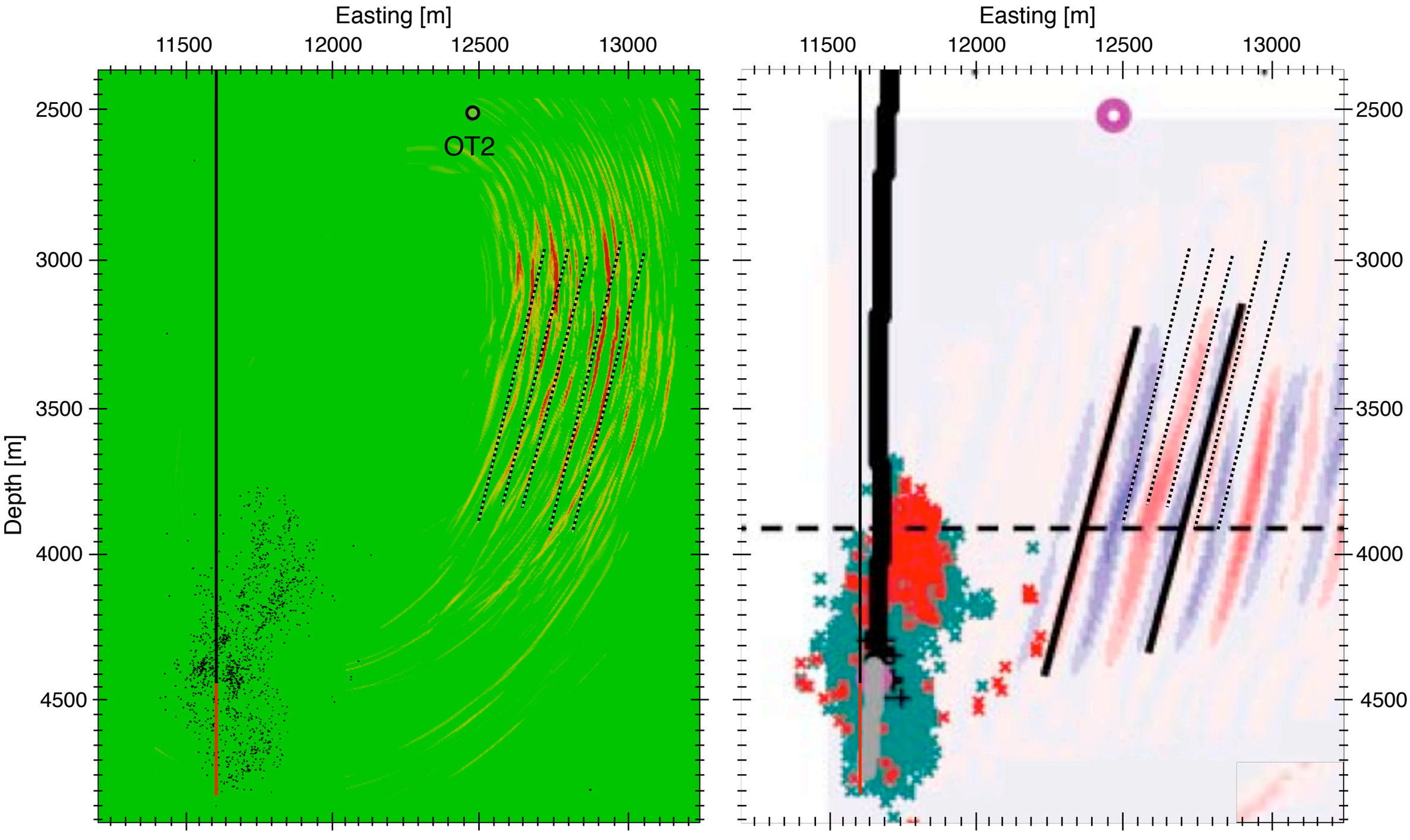


Dyer et al. (2008)

# Large scale fault system image: comparison

## Horizontal sections

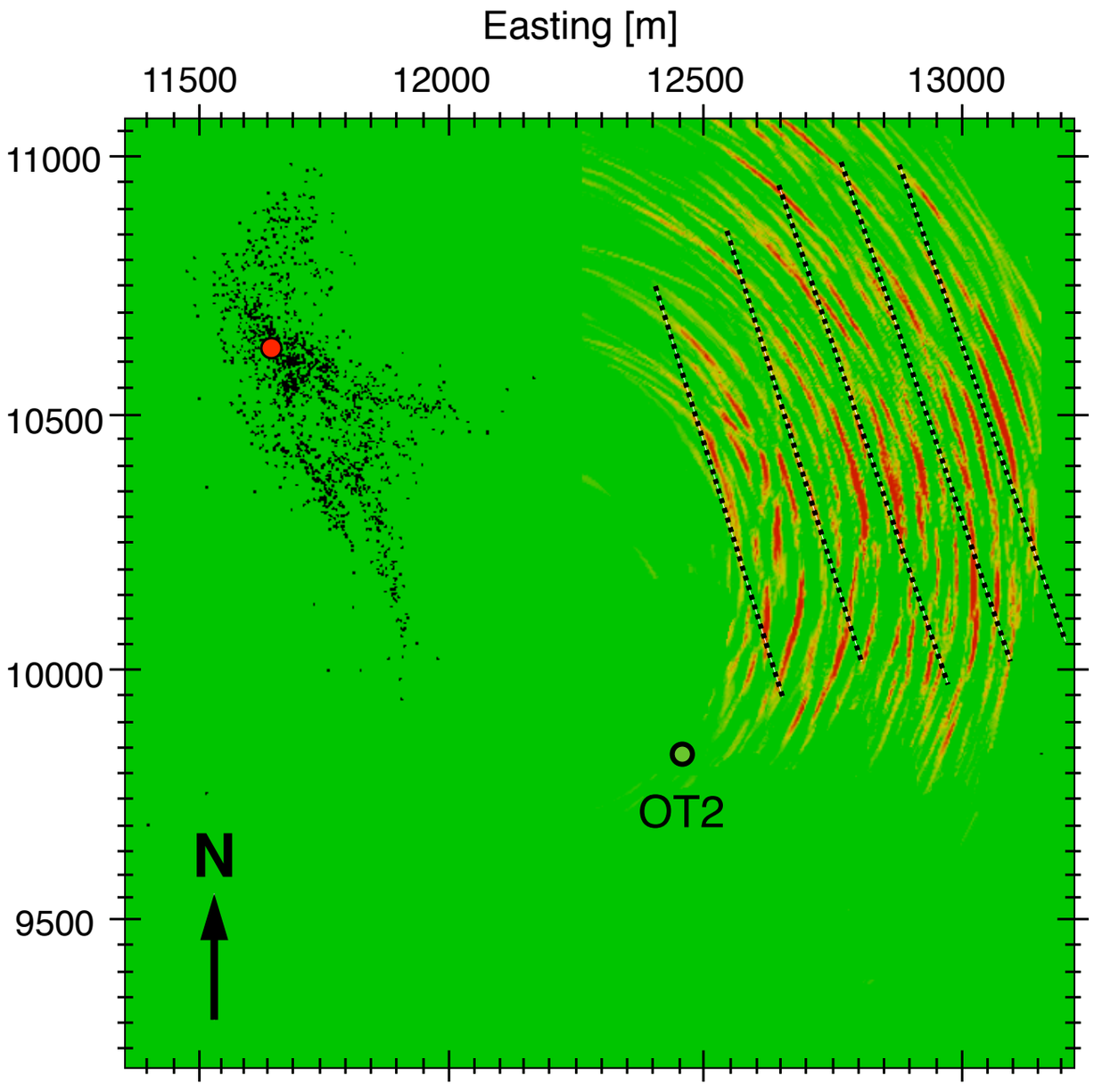


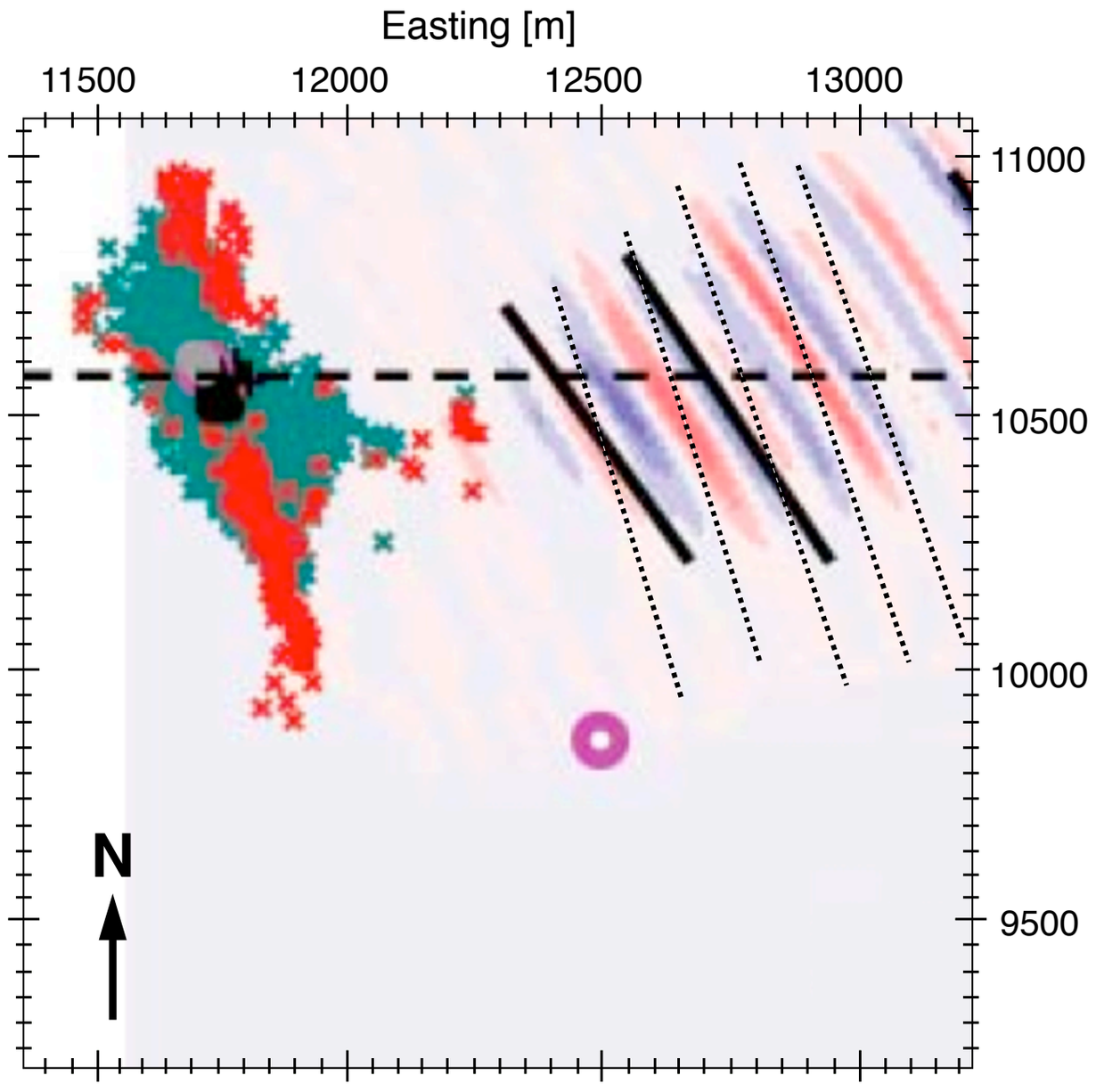


Dyer et al. (2008)

# Image of the microseismic cloud interior

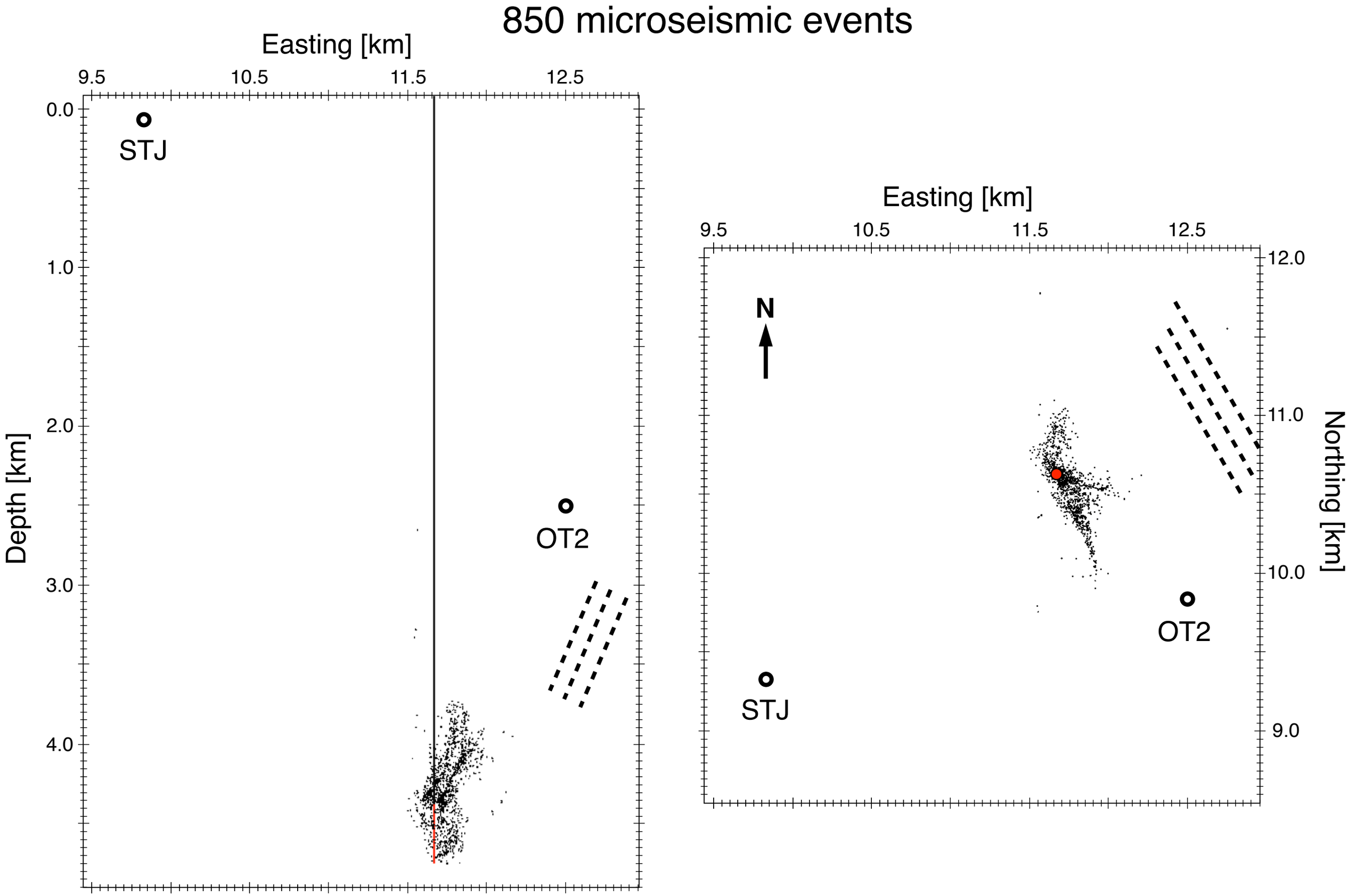

# Image of the microseismic cloud interior: imaging volume

1500x1500x1500 m,  4 m grid spacing

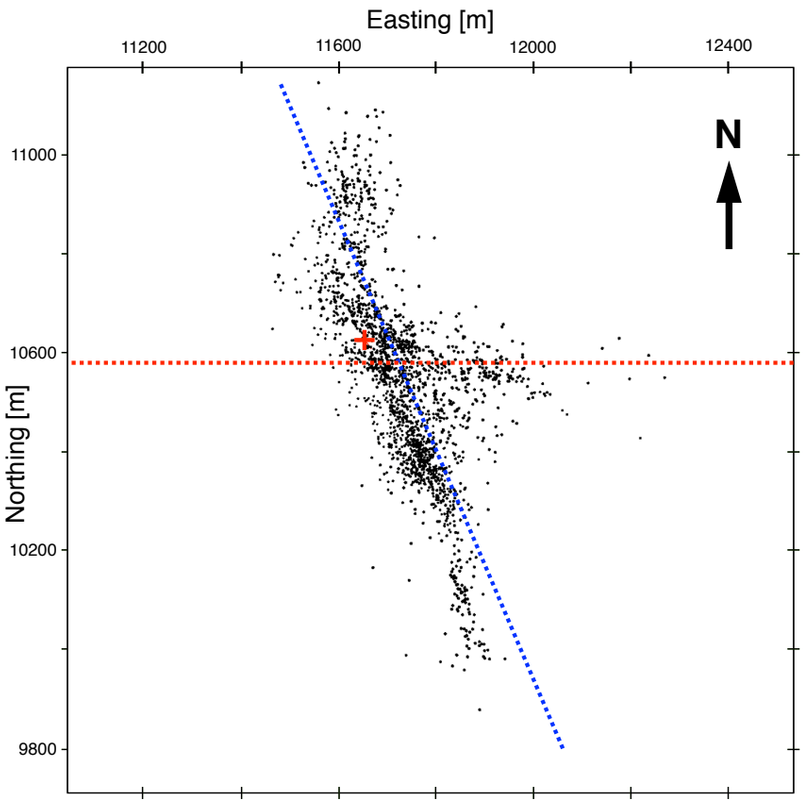


Horizontal view

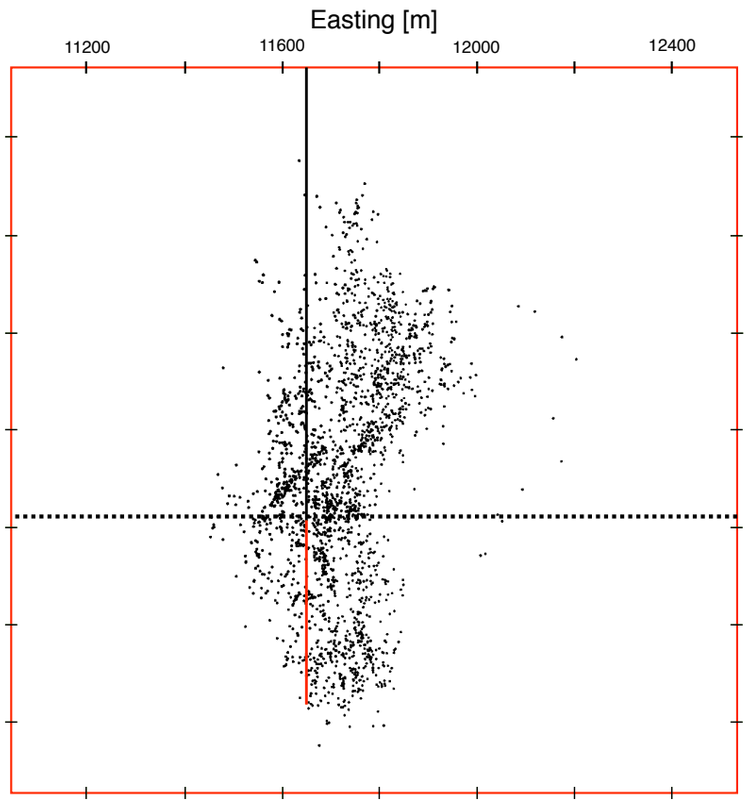


WE view

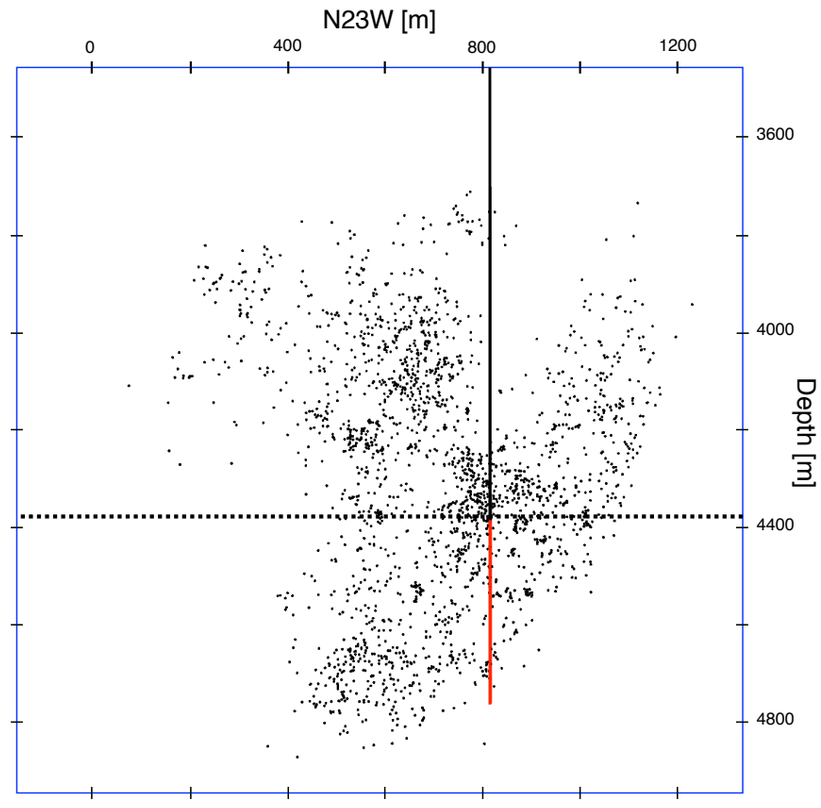


N23W view

# Image of the microseismic cloud interior: horizontal slice

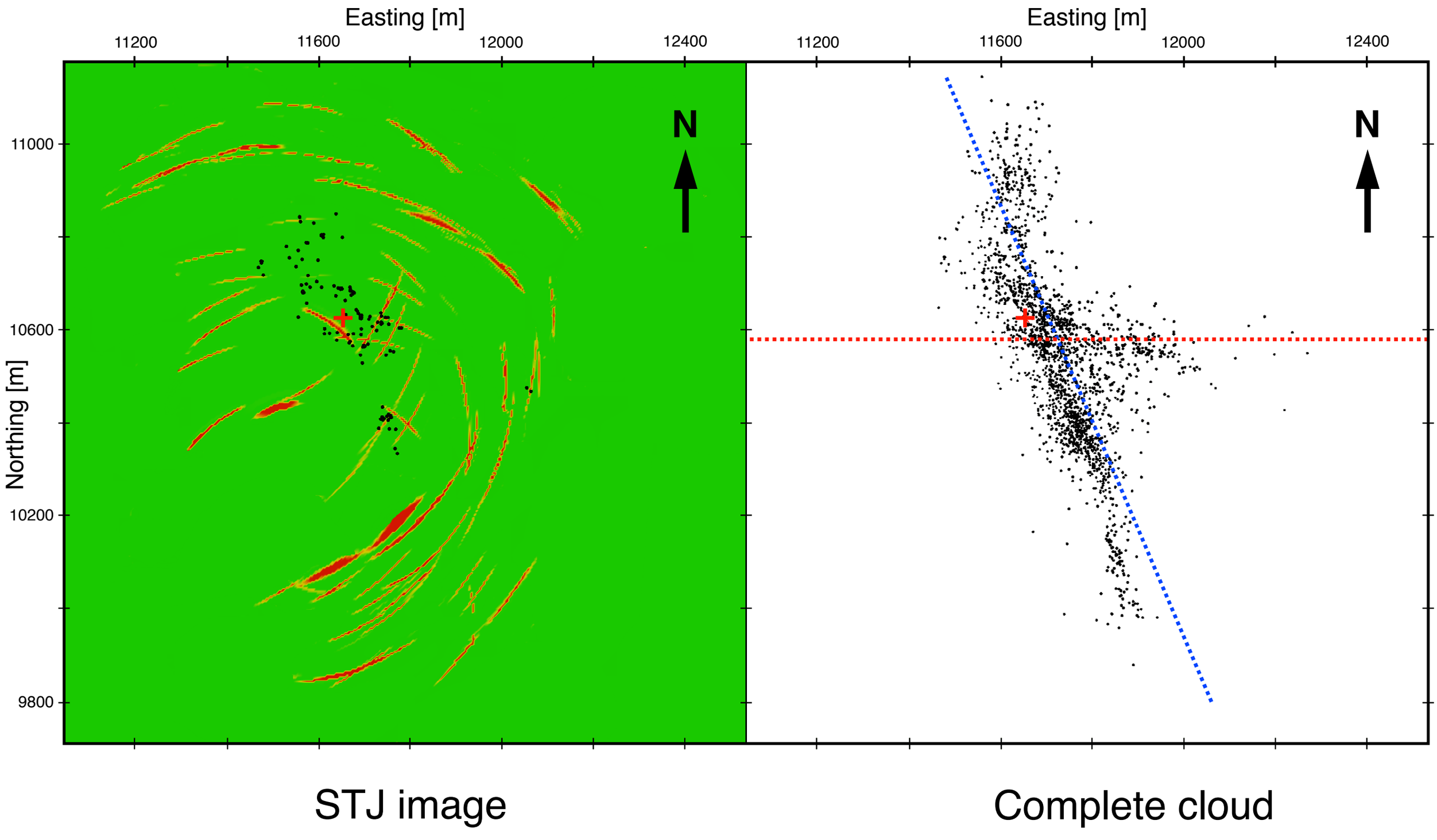

# Image of the microseismic cloud interior: WE slice

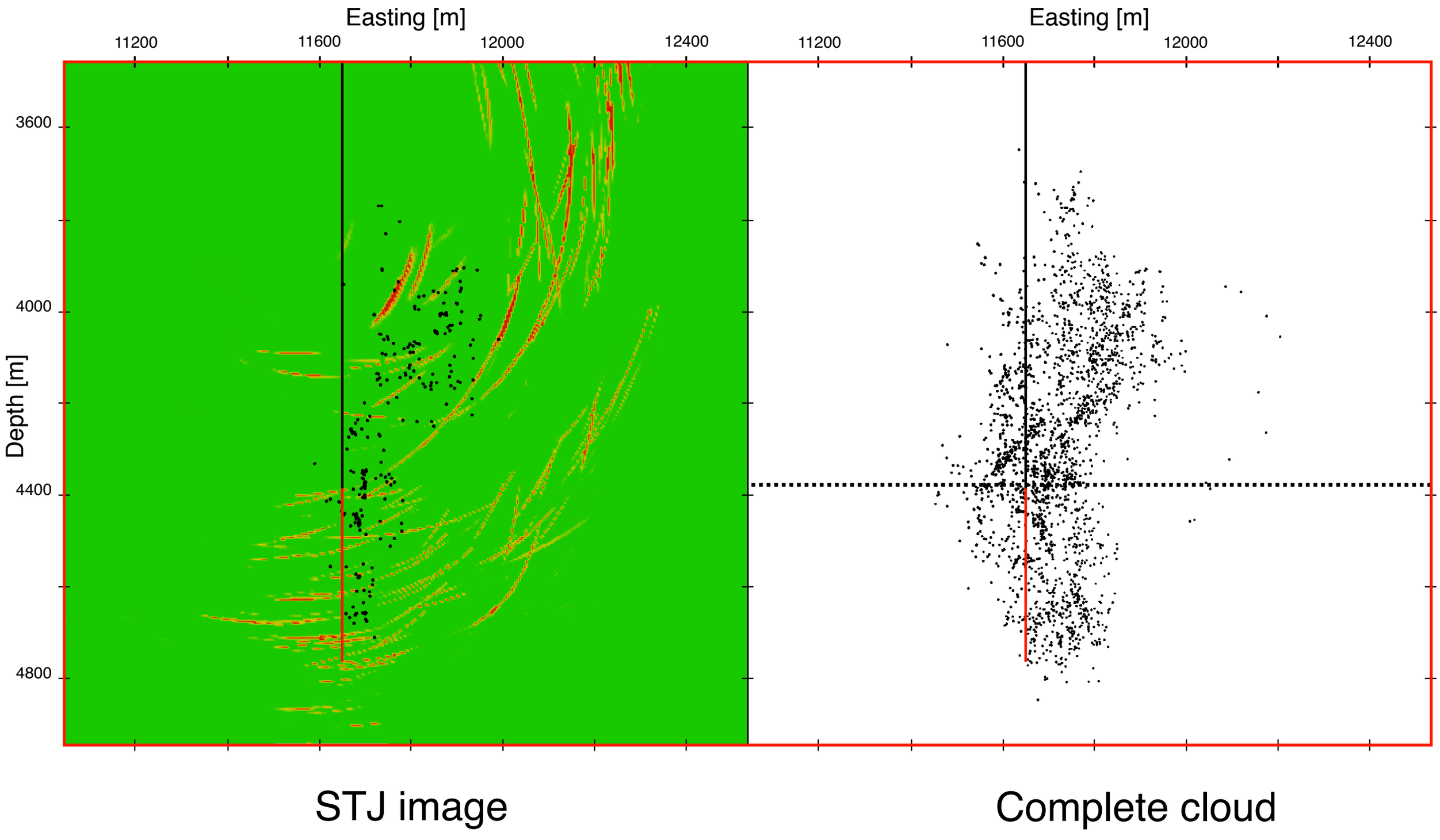

# Image of the microseismic cloud interior: N23W slice

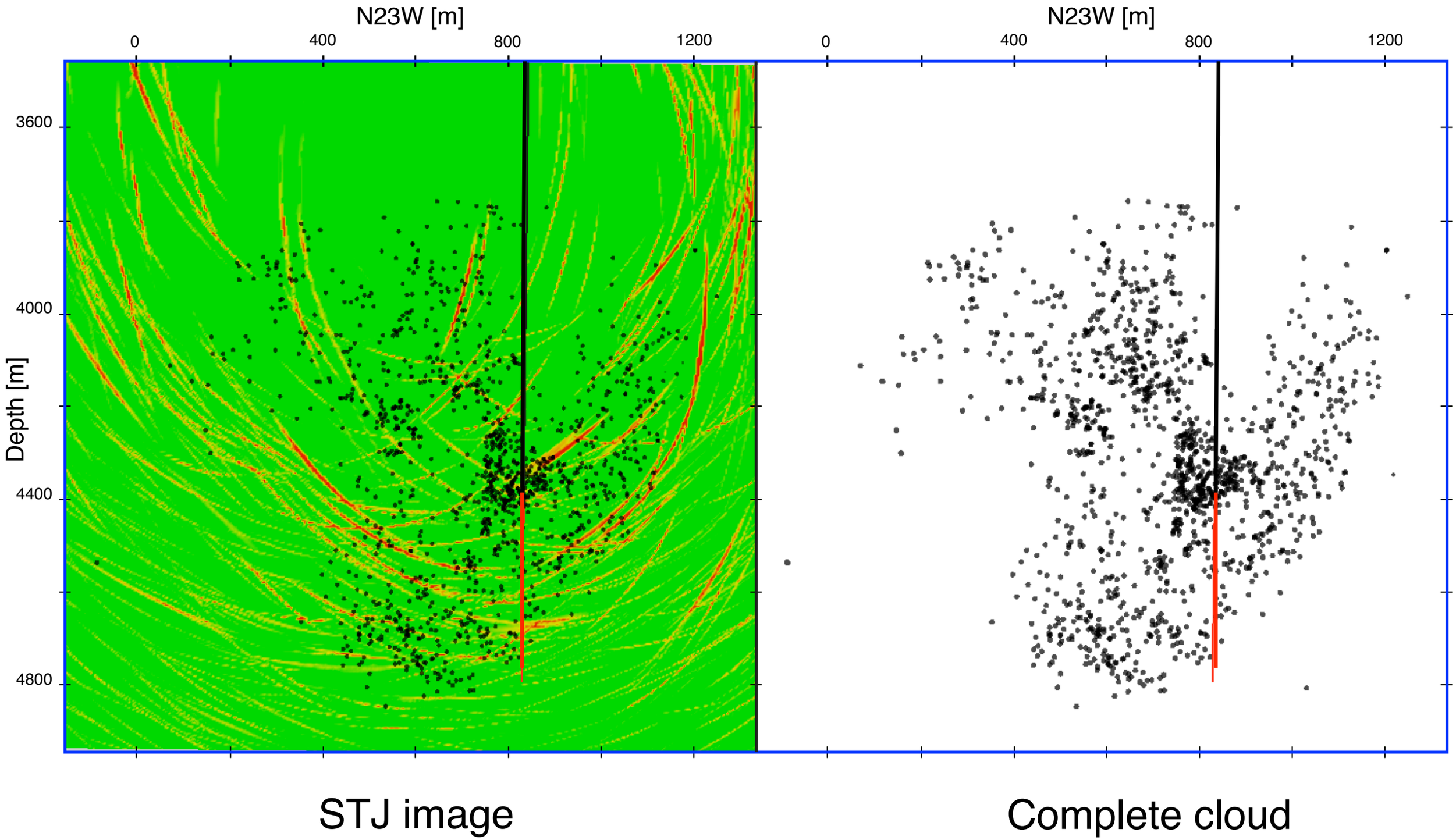

# Image of the microseismic cloud interior: comparison with the images from other stations

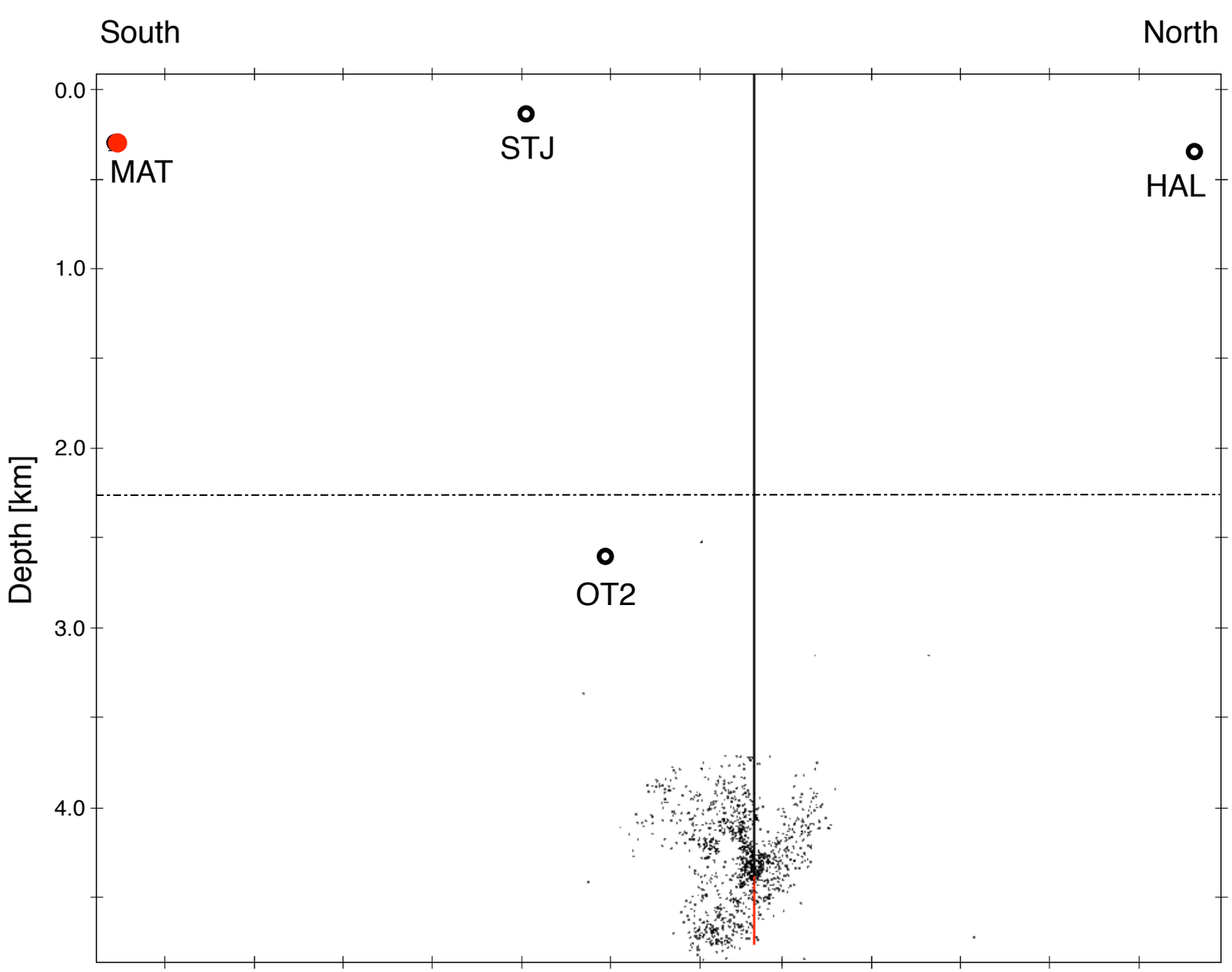


Side view

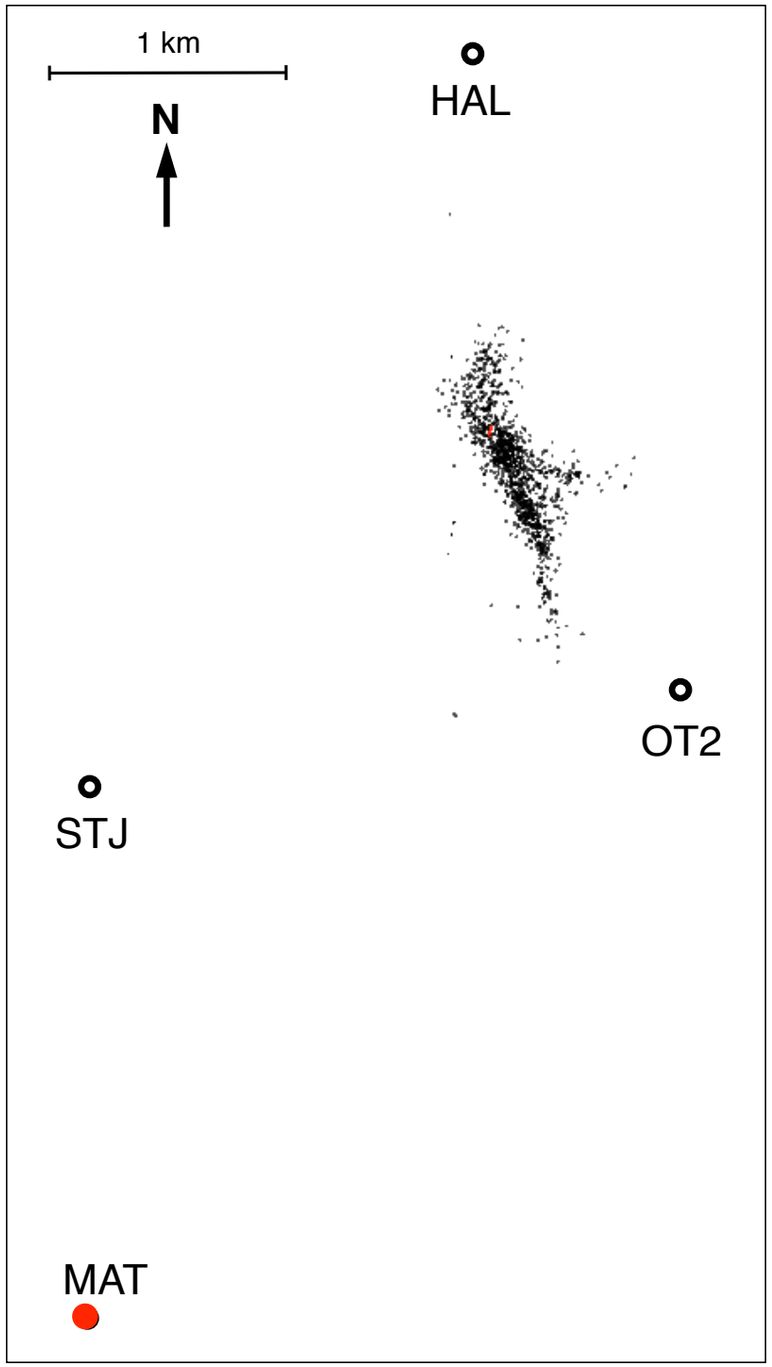


Map view

# Image of the microseismic cloud interior: N23W slice

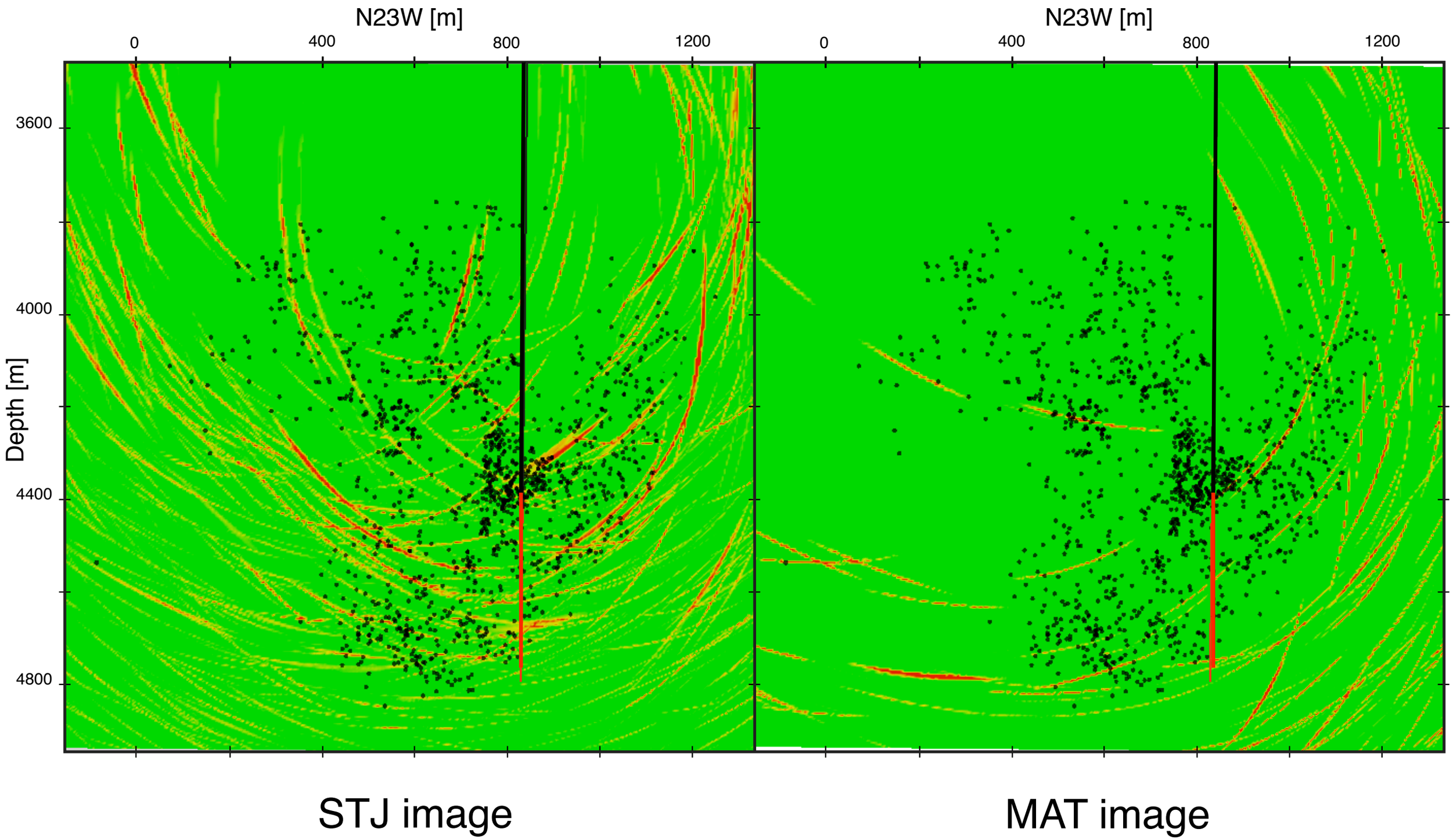

# Image of the microseismic cloud interior: comparison with the images from other stations

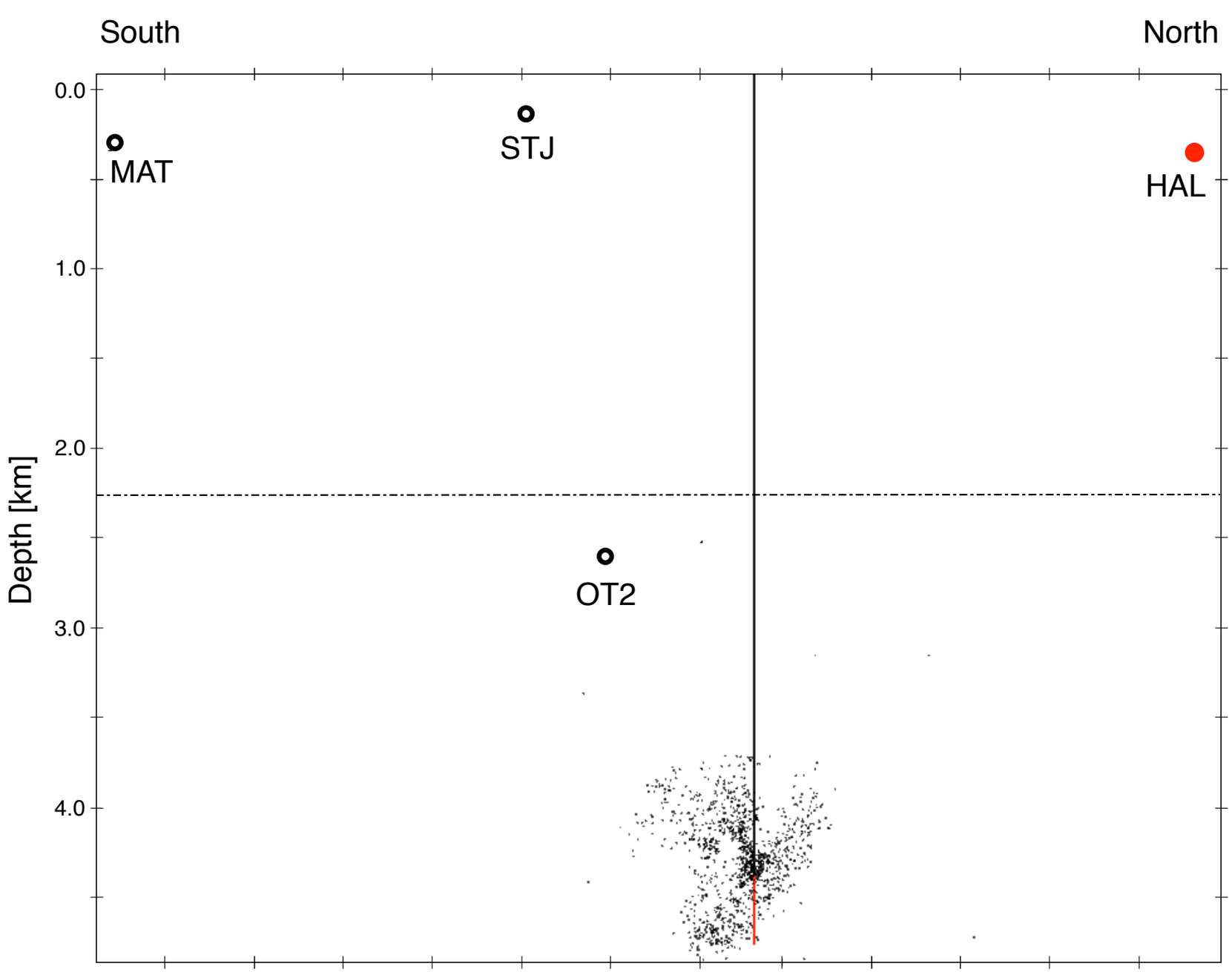


Side view

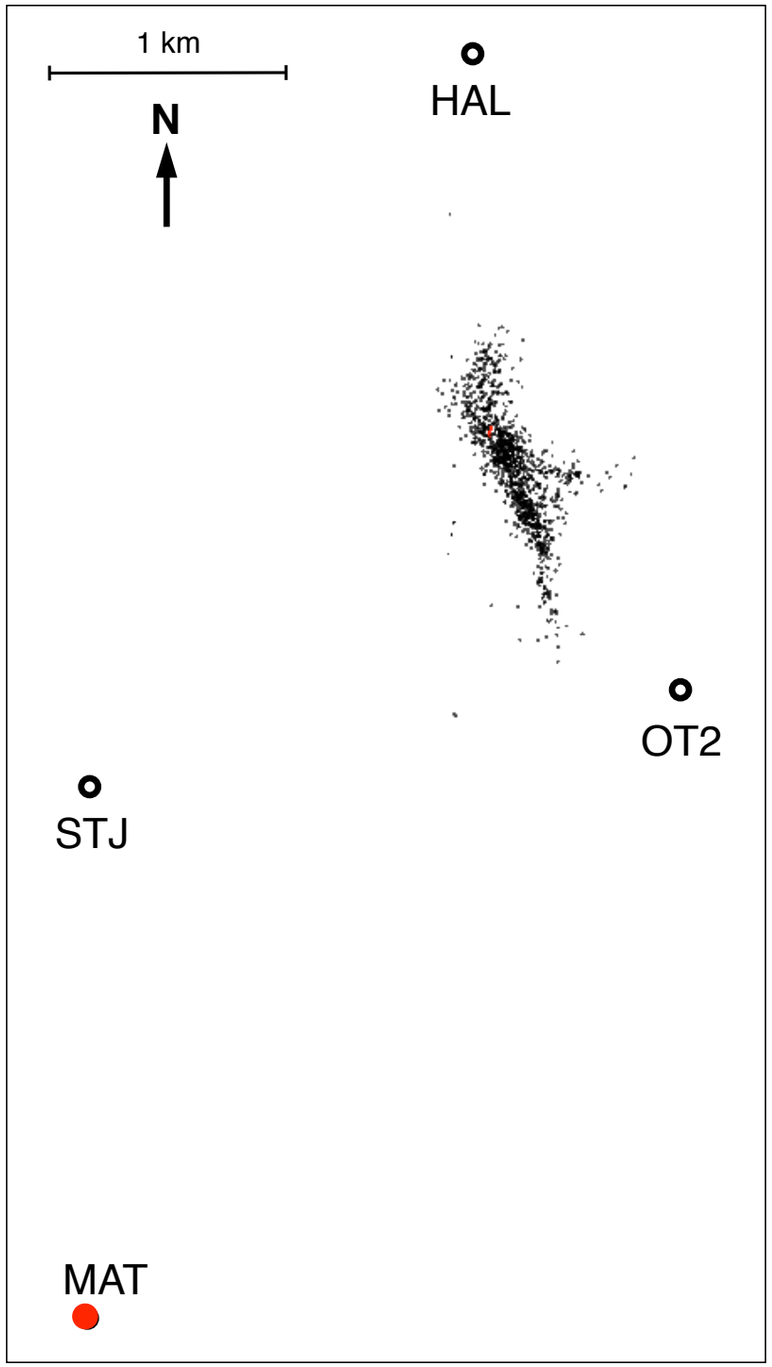


Map view

# Image of the microseismic cloud interior: N23W slice

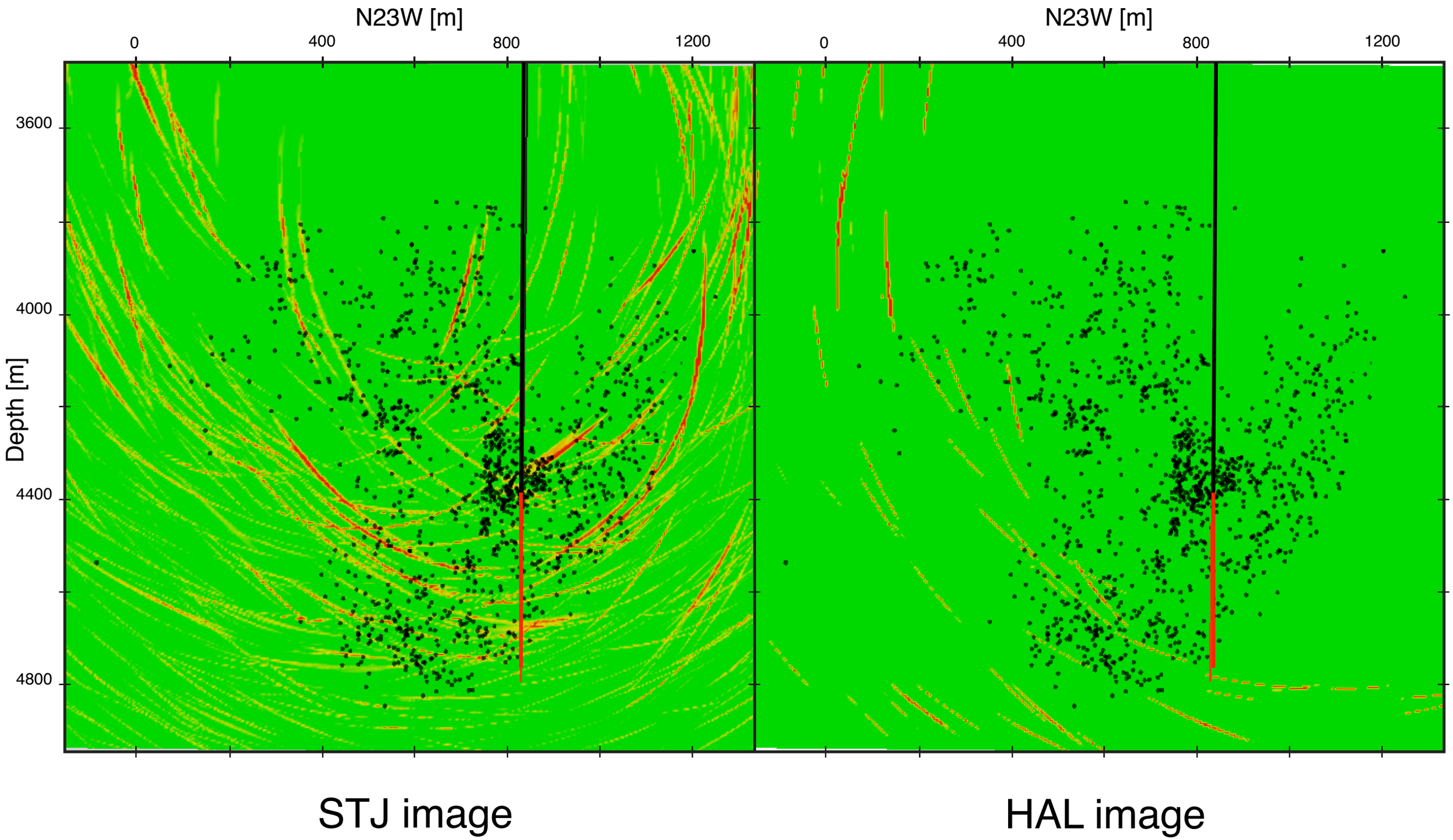

# Image of the microseismic cloud interior: N23W slice

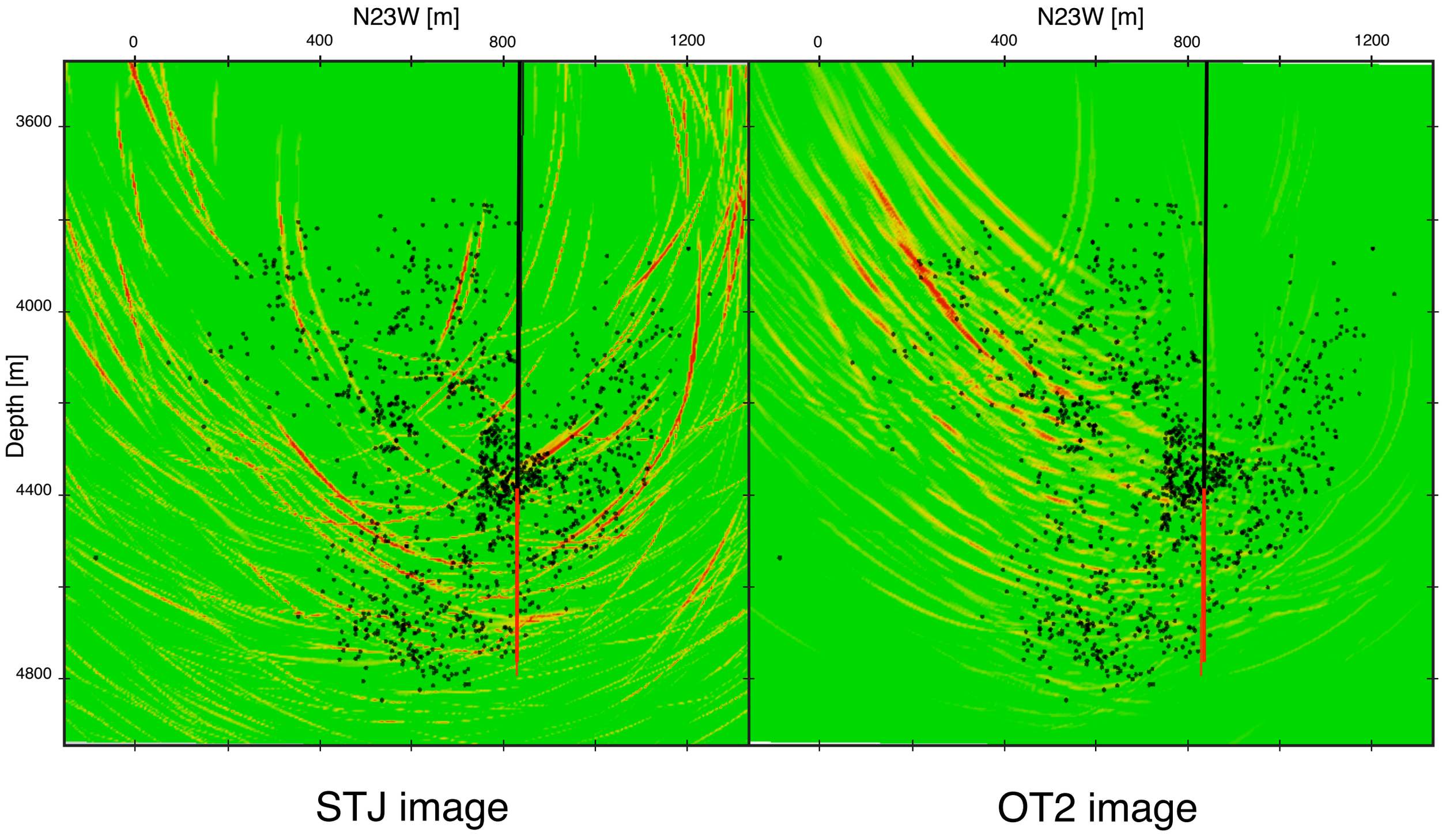

# Image of the microseismic cloud interior: 3D view

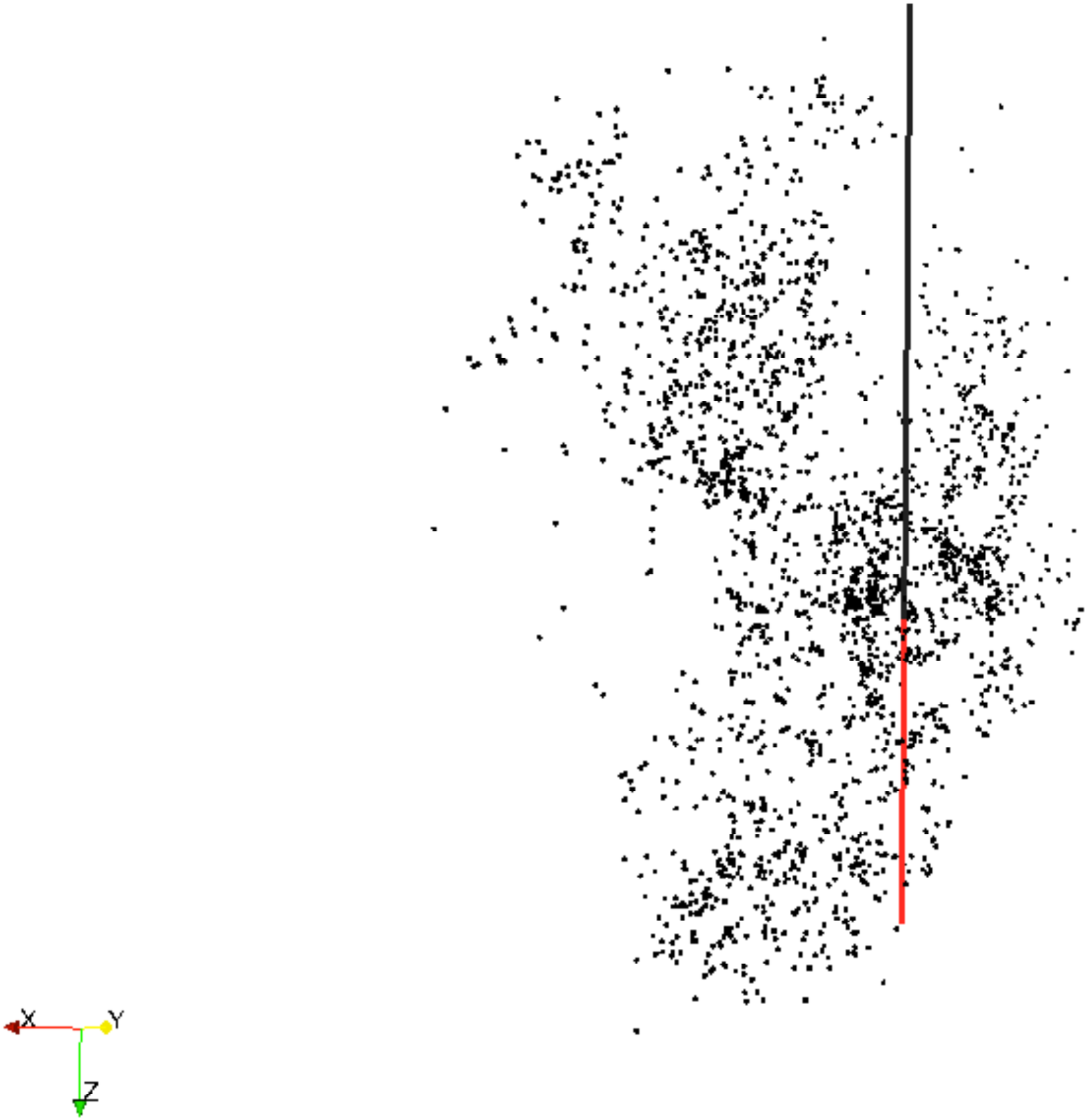

# Image of the microseismic cloud interior: 3D view

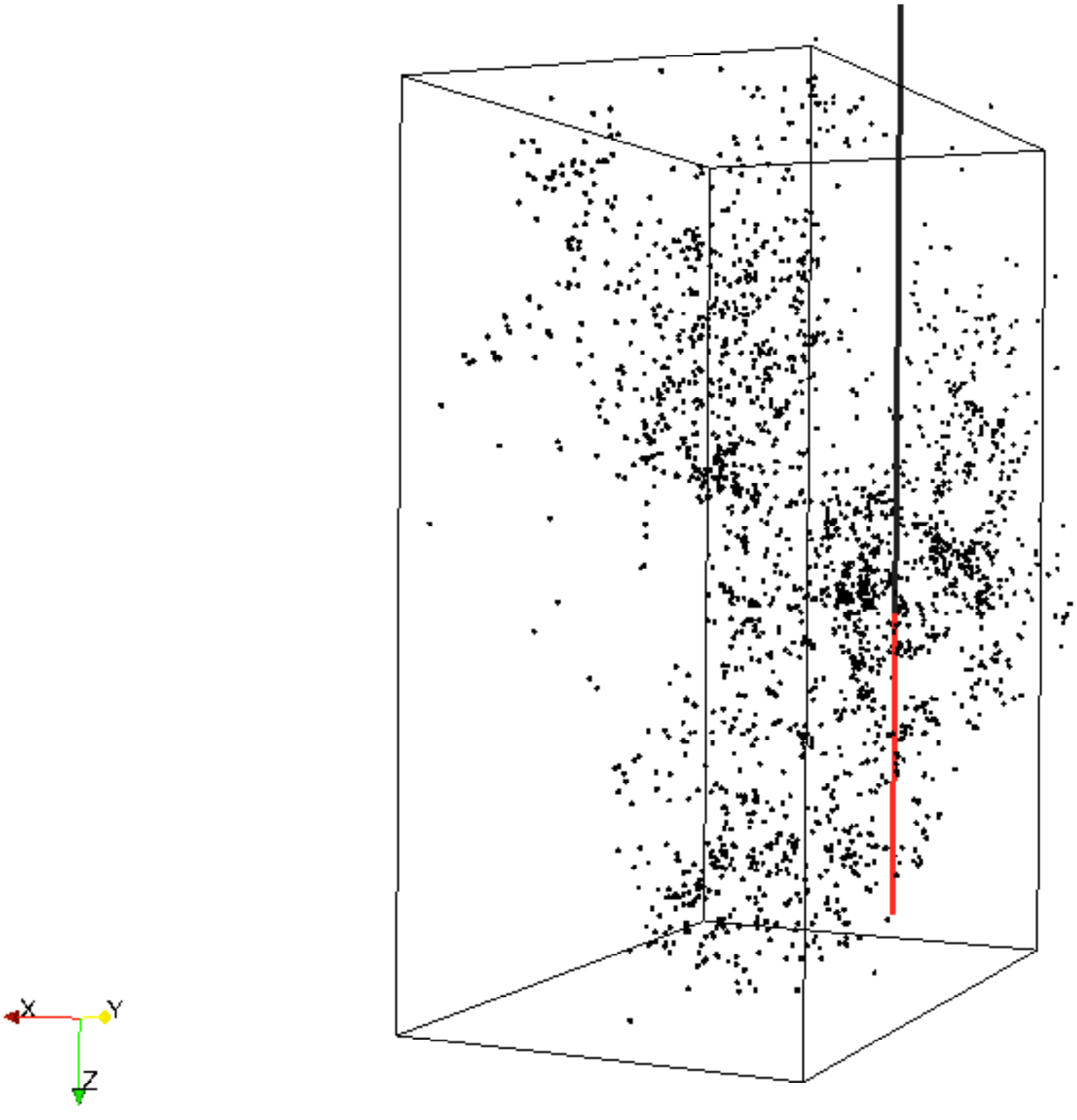

# Image of the microseismic cloud interior: 3D view

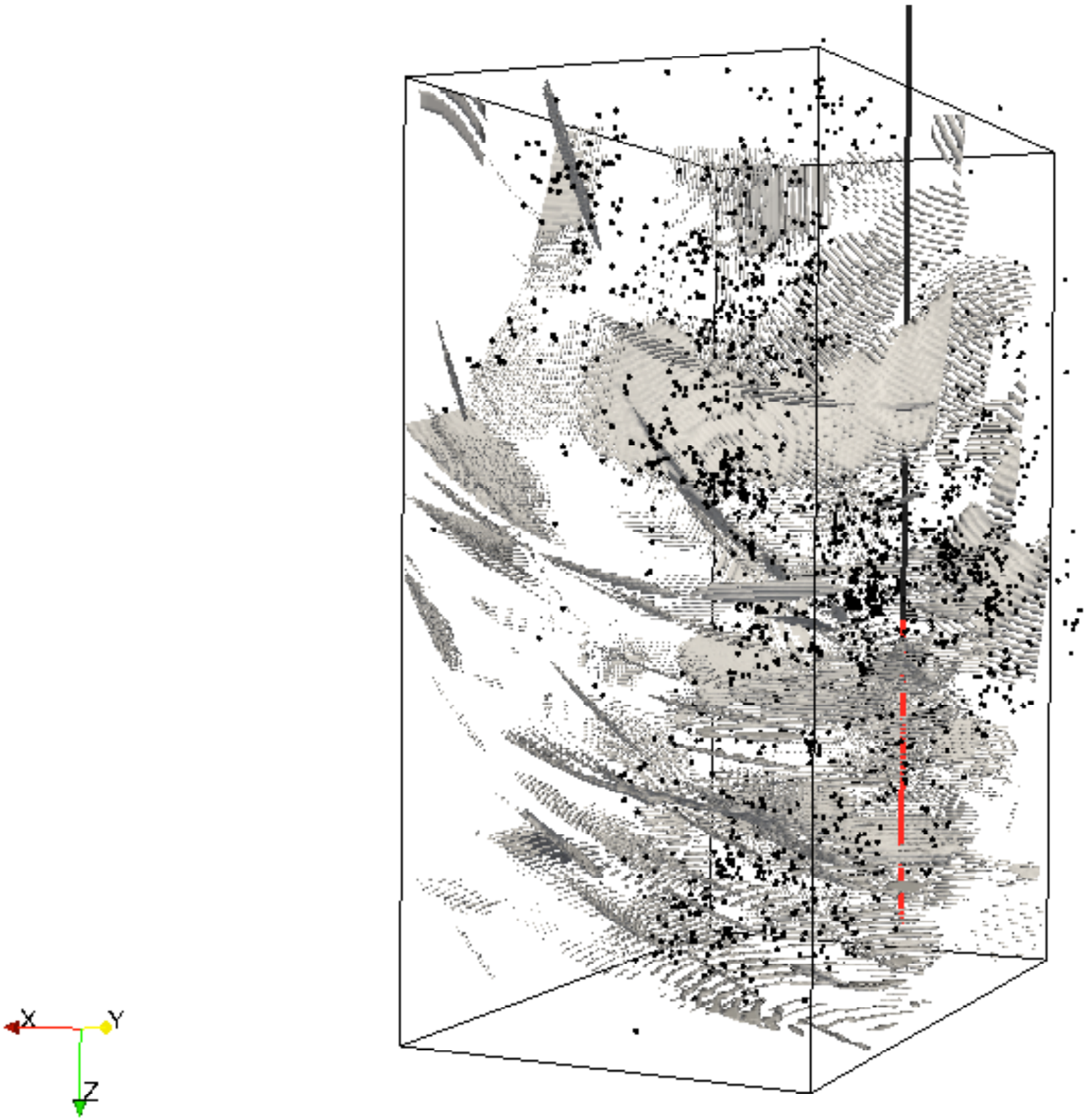

# Image of the microseismic cloud interior: 3D view

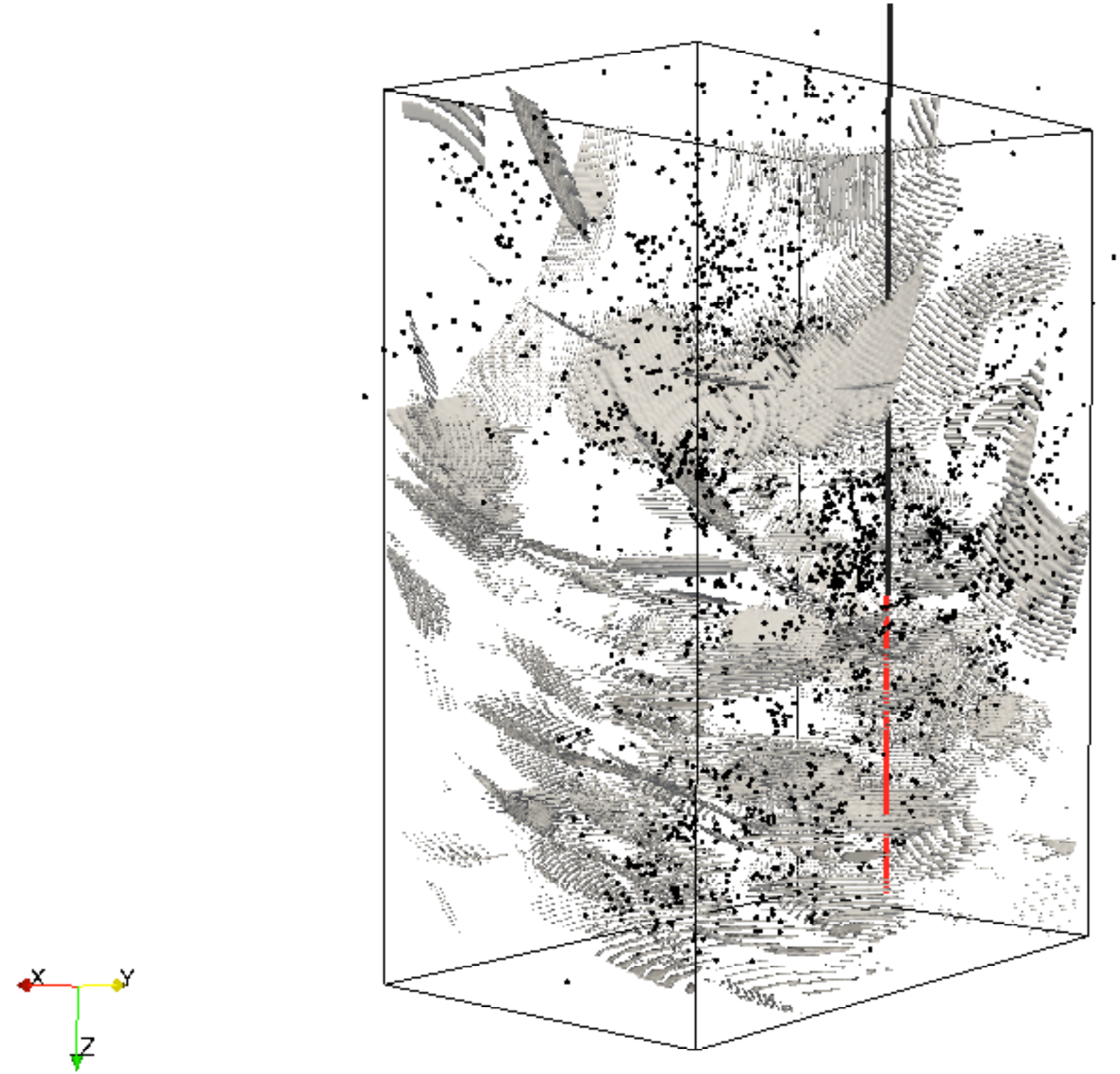

# Image of the microseismic cloud interior: 3D view

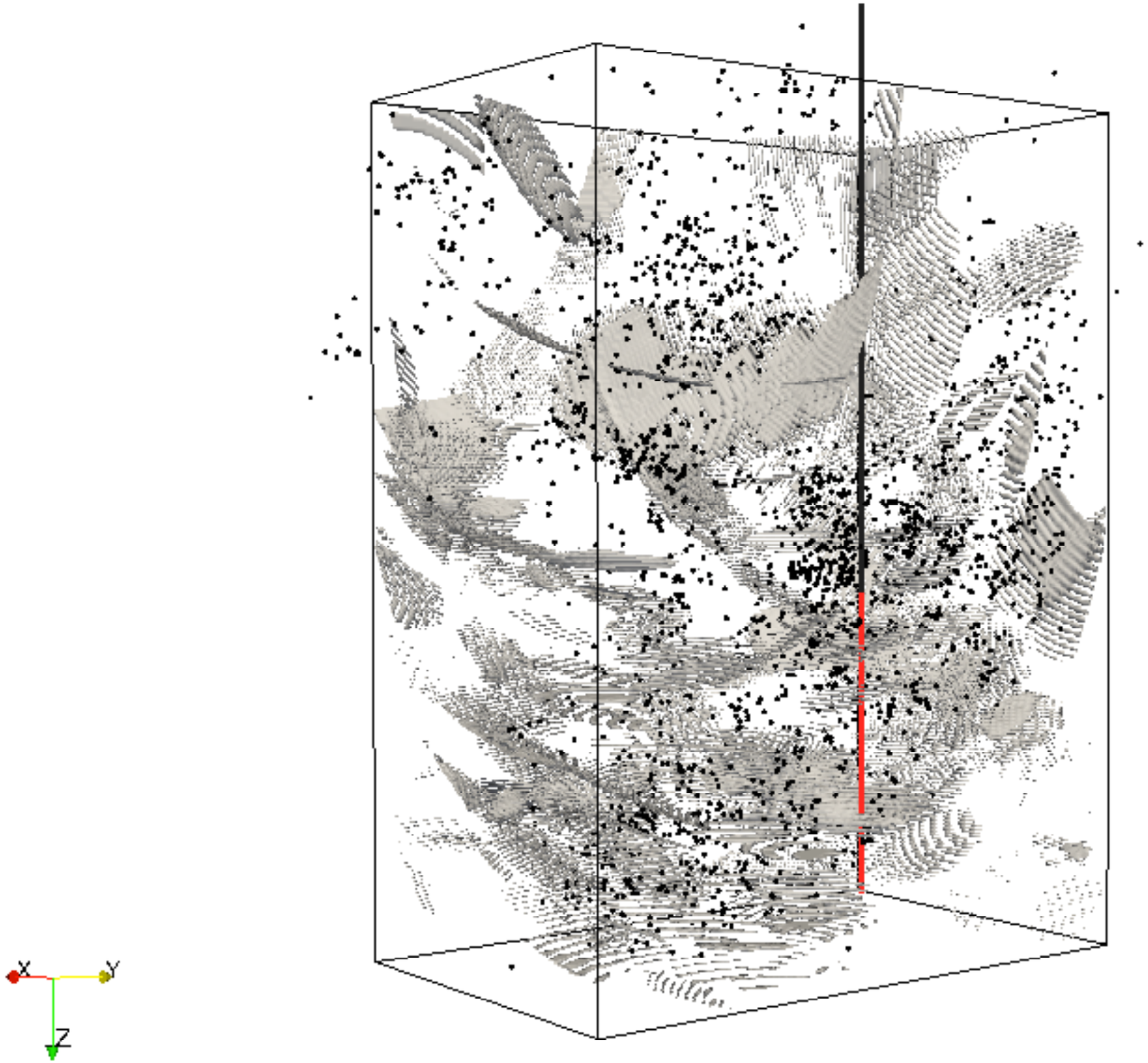

# Image of the microseismic cloud interior: 3D view

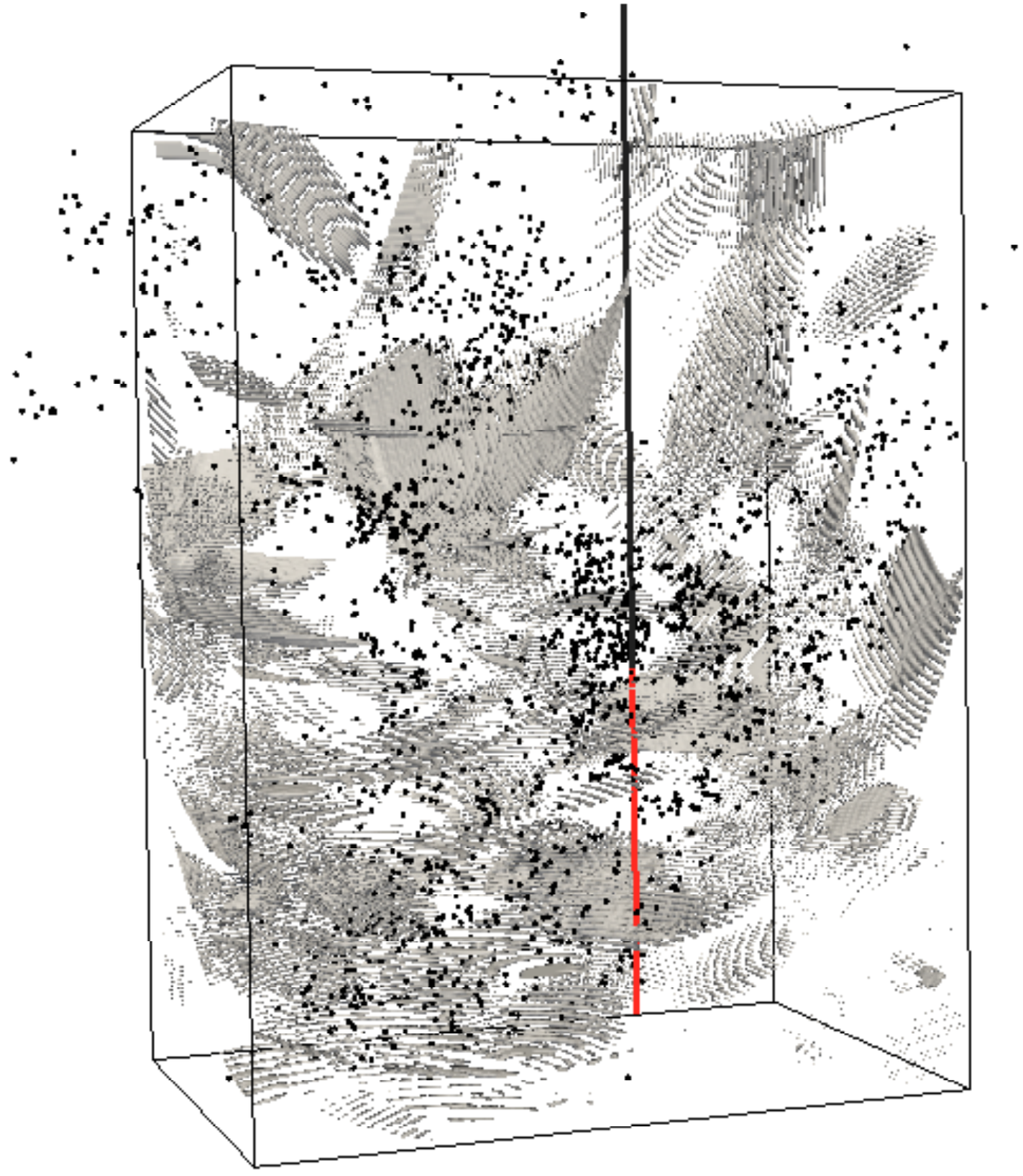

# Image of the microseismic cloud interior: 3D view

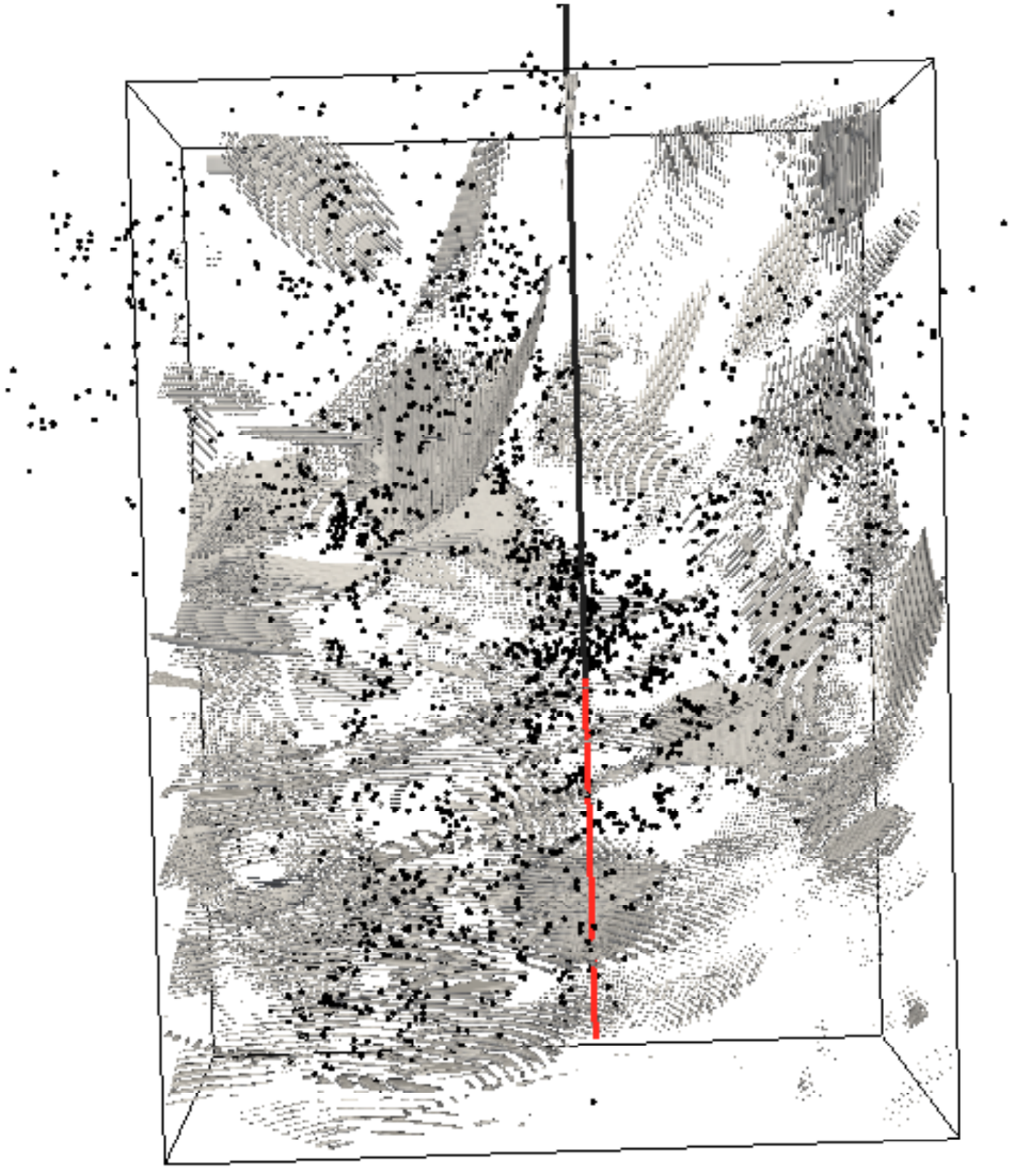

# Image of the microseismic cloud interior: 3D view

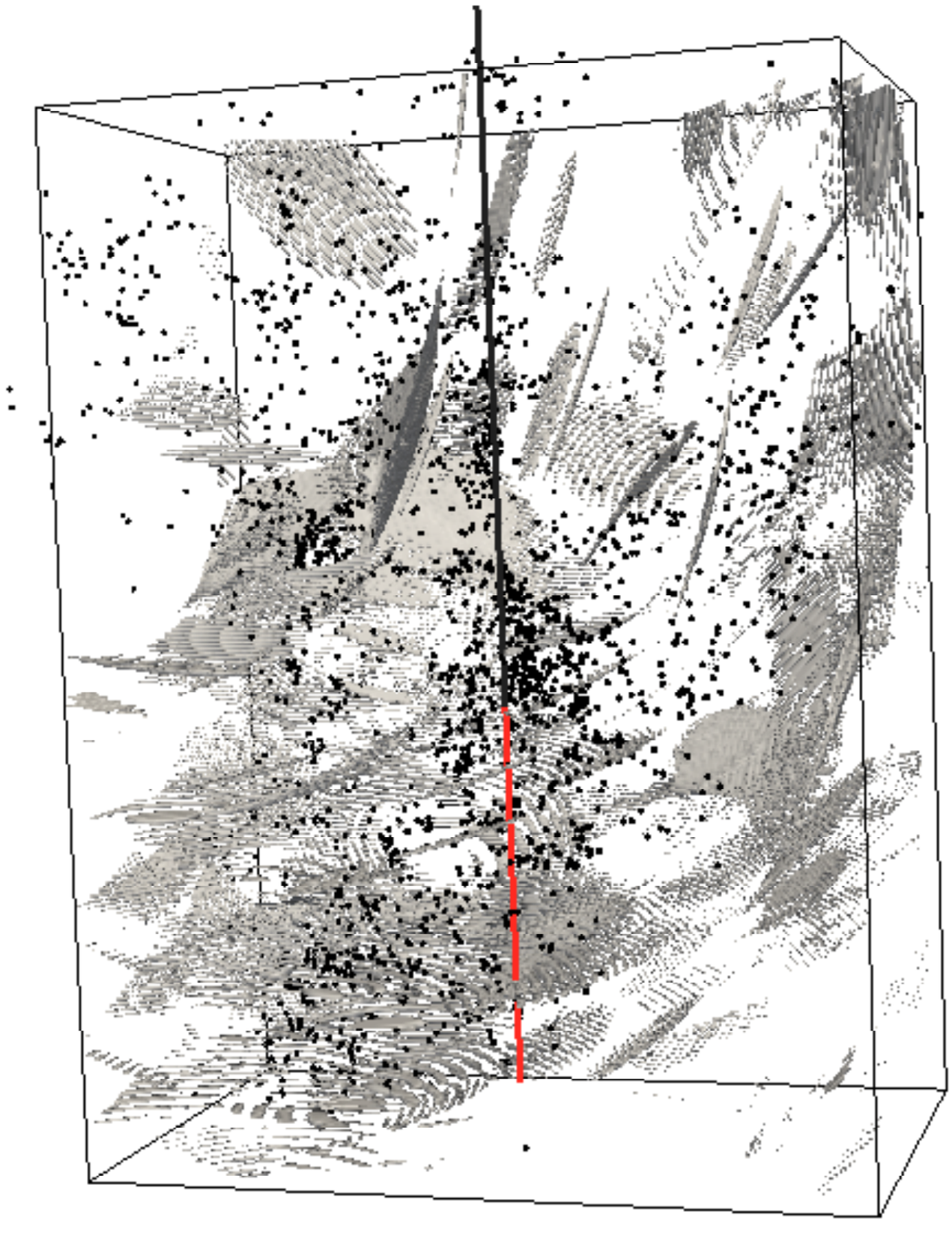

# Image of the microseismic cloud interior: 3D view

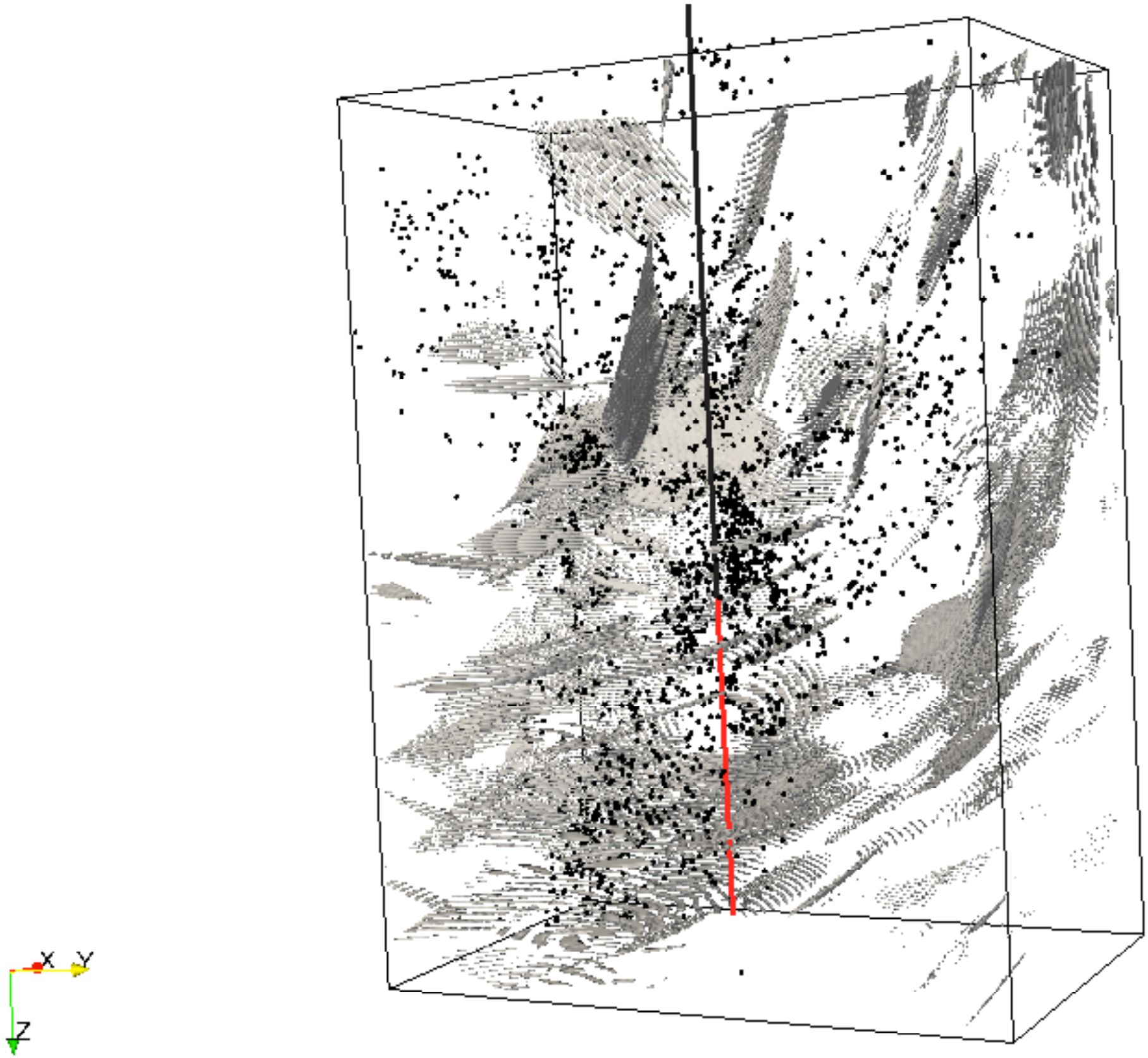

# Image of the microseismic cloud interior: 3D view

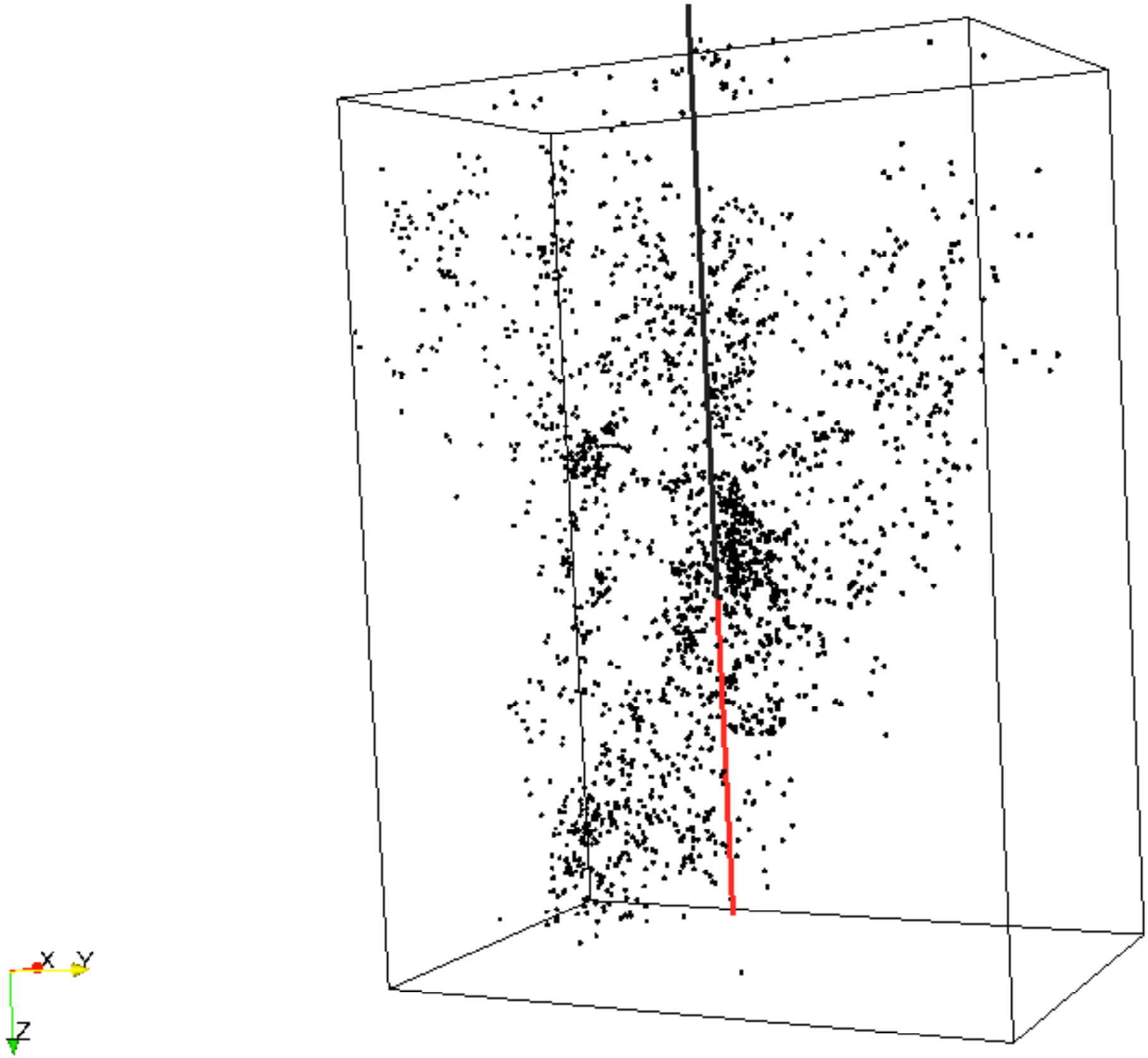

# Summary

- We have applied our microseismic reflection imaging approach to hydraulic reservoir simulation data
- Using the waveforms recorded at one geophone, we have constructed the image of large scale fault zone
- We have constructed the high resolution image of the microseismic cloud interior in the vicinity of the injection interval